

Hind-casting of High Resolution Atmospheric Fields
over Complex Terrain: *Model Initialization Issues*

Final Report

Project Number: WAC-03-220

Date: May 20, 2003

Submitted by: Bryan McEwen (M.Sc.), Dr. Peter L. Jackson

Submitted to: British Columbia Water, Land and Air Protection

ACKNOWLEDGEMENTS

The authors would like to thank Brendan Murphy (WLAP) for his efforts in acquiring the meteorological data needed to validate the simulations. Mr. Murphy's suggestions and comments on earlier drafts were also very useful.

We would also like to thank Chris Houser (WLAP) for doing significance testing on correlation coefficients, and for further analysis of the simulated fields. His work is presented in Appendix C.

Contents

1	Introduction	6
1.1	Rationale	6
1.2	Background: Numerical Weather Prediction	6
2	Modelling Strategy	8
2.1	Grids	9
2.2	Initialization and Nudging	15
3	Validation	15
3.1	Inherent Difficulties	15
3.2	Validation Times and Locations	16
3.3	Measures Used	18
4	Results	19
4.1	Modelling Experiences	19
4.2	Computer requirements	19
4.3	Surface Validation	20
4.3.1	Statistical Validation	20
4.3.2	Qualitative Validation	30
4.4	Upper Air Validation	36
5	Discussion	40
6	References	42
7	Appendix A: RAMS Initialization File	43
8	Appendix B: Windrose Diagrams	52
9	Appendix C: Significance Testing	61

List of Tables

1	RAMS Grid Sizes	9
2	Surface stations used for summer validation	17
3	Surface stations used for winter validation	17
4	Observed and Modelled Winds at Surface Station Locations (Summer Simulation, 1km resolution)	21
5	Observed and Modelled Winds at Surface Station Locations (Winter Simulation, 1km resolution)	21
6	Modelling Validation at Surface Station Locations (Summer Simulation, 1km resolution)	23
7	Modelling Validation at Surface Station Locations (Winter Simulation, 1km resolution)	24
8	Modelling Validation at Surface Station Locations (Summer Simulation, 3km resolution)	25
9	Modelling Validation at Surface Station Locations (Winter Simulation, 3km resolution)	25
10	Ensemble Validation at 1 km resolution (Summer Period), n = 2010	26
11	Ensemble Validation at 1 km resolution (Winter Period), n = 2251	26
12	Upper Air Validation using YLW upper air data (Summer Period)	37
13	Upper Air Validation using YLW upper air data (Winter Period)	37

List of Figures

1	RAMS Modelling Domain.	11
2	RAMS grid 4 (Thomson-Okanagan) at 3 km horizontal resolution. Topographical heights contoured in increments of 300 m.	12
3	RAMS grid 5 (centered near Kelowna) at 1 km horizontal resolution. Topographical heights contoured in increments of 200 m.	13

4	RAMS grid 6 (centered on Kamloops) at 1 km horizontal resolution. Topographical heights contoured in increments of 200 m.	14
5	Wind RMSE by hour of simulation for RAMS in a) HINDCAST mode, and b) FORECAST mode (summer simulation, 1km resolution).	28
6	Wind RMSE by hour of simulation for RAMS in a) HINDCAST mode, and b) FORECAST mode (winter simulation, 1km resolution).	29
7	HINDCAST modelled winds with observed wind vectors in red. Example of ‘good’ agreement on grid 5 during summer simulation	31
8	HINDCAST modelled winds with observed wind vectors in red. Example of ‘good’ agreement on grid 6 during summer simulation	32
9	HINDCAST modelled winds with observed wind vectors in red. Example of ‘poor’ agreement on grid 5 during summer simulation	33
10	HINDCAST modelled winds with observed wind vectors in red. Example of ‘poor’ agreement in grid 6 during summer simulation	34
11	Example Modelled and Observed soundings, Summer Simulation	38
12	Example Modelled and Observed soundings, Winter Simulation	39
13	Windrose diagrams showing observed and modelled surface winds for the duration of the summer simulation at MoF-2035 station.	53
14	Windrose diagrams showing observed and modelled surface winds for the duration of the summer simulation at MoF-2056 station.	54
15	Windrose diagrams showing observed and modelled surface winds for the duration of the winter simulation at MoTH-21091 station.	55
16	Windrose diagrams showing observed and modelled surface winds for the duration of the winter simulation at MoTH-33099 station.	56
17	Windrose diagrams showing observed and modelled surface winds for the duration of the summer simulation at WLAP-M116003 station.	57
18	Windrose diagrams showing observed and modelled surface winds for the duration of the summer simulation at EC-WJV station.	58
19	Windrose diagrams showing observed and modelled surface winds for the duration of the winter simulation at WLAP-M116003 station.	59

20 Windrose diagrams showing observed and modelled surface winds for the duration
of the winter simulation at WLAP-M112070 station. 60

1 Introduction

1.1 Rationale

The Province has expressed an interest in the development of a 5-year database of atmospheric conditions at high spatial and temporal resolution to support regulatory dispersion modelling activities and characterization of airsheds outside the Lower Fraser Valley. The focus of this study is to determine if there is a significant improvement in mesoscale model performance when the model is run in hind-cast mode using analysis fields every six hours, rather than real-time mode using forecast fields every three hours. As a test, a series of high resolution (1 km) simulations over the Thomson-Okanagan area of B.C. were conducted with the Regional Atmospheric Modeling System (RAMS). Simulated fields from both modelling strategies were compared to real observations. Bryan McEwen, in consultation with Dr. Peter Jackson of the University of Northern British Columbia (UNBC) was contracted to conduct the study. Atmospheric simulations were run on an SGI Origin 3400 computer, through the UNBC High Performance Computing facility.

1.2 Background: Numerical Weather Prediction

Prognostic Weather models simulate atmospheric processes by approximating the present state and then solving a set of non-linear partial differential equations that are based on dynamics, thermodynamics, mass continuity and conservation of variables such as moisture. These equations are not analytically solvable, and approximations must be used to determine solutions. Numerical methods such as finite differencing are used for this purpose. A finite difference scheme approximates differential equations with a set of algebraic difference equations for values of the tendencies (spatial gradients) of various field variables. The tendencies are determined by solving the difference equations. By extrapolating the tendencies ahead in time by a small increment, an estimate for values in the next time interval are obtained. The process then repeats for the next time step (e.g. Holton, 1979). These equations are supplemented with a selection of parameterizations for those processes that are able to influence atmospheric evolution at scales smaller than the model is able to resolve. These include solar and terrestrial radiation, moist

processes such as cloud development and precipitation, kinematic effects of terrain, sensible and latent heat exchange and turbulence.

Prognostic models utilize a grid system to represent the section of atmosphere being studied. Each grid point contains a value of a variable for a volume of the surrounding air, called a 'grid cell'. Computer processing time is strongly linked to the size of the domain being modelled, and the grid cell sizes within. Numerical models are classified by the scales of motion they simulate. A synoptic-scale model is used to forecast weather and typically has very large grid cells. A mesoscale model uses smaller grid cell spacings with the intent to resolve smaller-scale motions. RAMS, a well-known mesoscale model, has used horizontal grid spacings as small as 100 m to simulate thunderstorms (e.g. Pielke *et al*, 1992).

Models such as RAMS are considered research models, because they have numerous optional physical algorithms. Each model is actually a system that incorporates many separate, stand-alone components that are models in themselves (Cox *et al*, 1998a). This 'plug compatibility' facilitates both usefulness in research and ease of changing or adding model features. RAMS has been compared favourably to other mesoscale models such as MM5 in the past (e.g. Cox *et al*, 1998b). Observational data analysis is a large component of any atmospheric model. The data required by the model must be processed before it is used, so that errors or problematic gradients do not lead to imbalanced numerical conditions (Stull, 1995). It is common for mesoscale models such as RAMS and MM5 to use large gridded datasets that are produced by synoptic scale models (such as the Eta 90 km model used in this study) to produce the initial conditions used to begin a simulation. These large-scale gridded analysis and forecast fields are regularly produced by several atmospheric models, and are freely available through the internet. The data are accessed for the area being modelled, and are interpolated to the horizontal and vertical coordinates of the mesoscale model grid as objective analysis fields (e.g. Pielke *et al*, 1992). Although surface or upper-air meteorological station data can be blended in to the objective analysis fields using weighted averaging, the fields themselves are enough to initialize the model and 'nudge' its predictions at regular time intervals. Nudging uses Newtonian relaxation to force model variables to approach the values of the objectively analyzed fields. The nudging can occur at the lateral boundaries, through the center, and at the top of a model domain; with the strength of the process being set by the operator. Generally, stronger nudging is used along lateral boundaries and

relatively weak nudging is used through the center of a grid. Strong nudging at the center of a grid tends to overwhelm the model physics; leading to an interpolated field (from the synoptic-scale input) rather than a prognosed field (Walko and Tremback, 2002).

When high model resolution is required, for example when smaller scales of motion need to be revealed, grid nesting can be used. A nested grid, with higher spatial resolution, occupies a region within the domain of its coarser ‘parent’ grid. Any number of nested grids may be used, with the only practical limit being available computer memory. The use of nested grids greatly increases the number of calculations the computer must perform during a model run. This is because a smaller grid spacing necessitates a much smaller interval of time that the model is able to step ahead (known as the ‘timestep’) when calculating the future atmospheric state. The model must take several smaller timesteps in its calculations within a nested grid for every time step taken of its parent grid. For RAMS, there is two-way communication of all prognostic variables between a nested grid and its immediate parent (Walko and Tremback, 2002). Fine grid values are averaged to replace the coarse grid value which they surround.

2 Modelling Strategy

The Regional (90 km) Eta model analysis and forecast fields, which are archived at UNBC, were used to initialize and guide RAMS model simulations. The Eta model is currently used in 19 different countries for research and operationally in 8 countries (including the U.S.). The development team currently working on the model resides at The Centers For Environmental Prediction (NCEP). Several versions of this model exist, each with a different level of resolution. The 90 km version is continuously run over a large domain including all of North America; which makes it a useful resource for mesoscale models such as RAMS.

Both modelling strategies tested in this work used RAMS to simulate the atmosphere. RAMS in hind-cast mode (designated ‘HINDCAST’) used *analysed* 90 km Eta model fields to initialize and nudge simulations. These fields are produced by Eta from available observations every six hours. Nudging for this model configuration therefore occurs at six hour intervals. RAMS in forecast mode (designated ‘FORECAST’) used analyzed 90 km Eta fields for initialization and *forecast* fields for nudging. The Eta forecast fields are produced at 0 UTC every day in intervals of three

hours. Nudging for this model configuration occurs at three hour intervals.

The region of interest to be studied in this work was chosen by the Ministry of Water, Land and Air Protection (WLAP) to encompass the Thomson-Okanagan area of British Columbia. One of the reasons this region was chosen was that it possesses both an upper-air meteorological station (at Kelowna) and many surface stations that can be used to validate modelling efforts. Two two-week periods from June 12-24, 2002 and January 28 - February 10, 2003 were chosen to simulate with RAMS. The summer period contained intervals of high ground level ozone concentrations and the winter period contained intervals of high particulate matter concentrations. Both periods had calm days when wind speeds were low.

To determine which modelling strategy produces higher quality meteorological fields, the RAMS fields were validated with hourly surface station observations throughout the domain and with 12Z (evening) upper air observations at Kelowna YLW. The validation exercise also details some of the characteristics of the high resolution mesoscale model fields produced.

2.1 Grids

A RAMS modelling domain with 6 nested grids was created to produce the meteorological fields for this study. Table 1 shows the extent and resolution of the 6 grids used in each simulation.

Figure 1 gives an indication of the geographic boundaries of each grid.

Grid	Grid Cell Spacing (km)	Number of Grid Points in x	Number of Grid Points in y	Parent Grid	Grid S.W. Corner (lat/lon)	Grid N.E. Corner (lat/lon)
1	81	60	60	-	26.1,-170.0	71.3,-69.2
2	27	62	62	1	42.1,-129.6	56.7,-106.1
3	9	62	62	2	47.5,-123.3	52.4,-115.6
4	3	74	83	3	49.2,-121.4	51.4,-118.3
5	1	62	98	4	49.43,-119.90	50.36,-119.04
6	1	62	62	4	50.45,-120.96	51.00,-120.11

Table 1: RAMS Grid Sizes

Several criteria were used to select the size and resolution of the six grids. The coarse grid (grid 1) must be large enough to resolve the significant synoptic features influencing regional flow, and the innermost grids (5 and 6) must have fine enough resolution to adequately represent the effect local topography has on winds near the surface. Grid 1 is likely more than large enough to capture the regional flow. This grid was included because its horizontal spacing (81 km) is close to that of the Eta model fields that were used for initialization and nudging.

It is physically difficult for the model to step down grid size in large increments (e.g. Walko and Tremback, 2002), so the nesting ratio between grids was set at three. Note in Table 1 that both of the 1 km grids are nested within grid 4. The height of each grid cell, for all six grids, was set at an initial value of 25 m for each grid. Previous studies have shown that vertical spacing in a mesoscale model must be 25 m or less near the earth's surface in order to account for terrain forcing in complex topography (e.g. McQueen *et al*, 1995). A stretch factor was also applied, which caused this vertical spacing to gradually increase with distance from the surface.

The size and spacing of the inner grids is directly related to demands on computer cpu time. Presently, choosing the inner grids with horizontal spacings less than 1 km would be very computationally expensive. In fact, very few mesoscale modelling initiatives to date have used inner grid spacings as small as those used in this study.

USGS datasets of topographical heights and vegetation class were used to simulate the terrain in the model. These datasets are at a resolution of 30 arc-seconds (about 1 km), making them suitable for the inner domains. There are several different topographical 'smoothing' options in RAMS to use with the topographical dataset. In areas of complex terrain, large gradients in terrain heights can cause numerical instability in a model run. Some smoothing must be performed on the terrain to reduce the likelihood of numerical instability, but too much smoothing weakens the influence topography has on modelled boundary layer features. Reflected envelope orography was chosen within the model, as this scheme best preserves valley depths and ridge heights (Walko and Tremback, 2002). Figures 2, 3, and 4 show the topography of the inner grids 4, 5 and 6, with the locations of the surface meteorological stations that were used in model validation. A RAMS input file is presented in Appendix C which details all of the model settings for this study. Model settings for HINDCAST were identical to those for FORECAST, with the exception of nudging frequency.

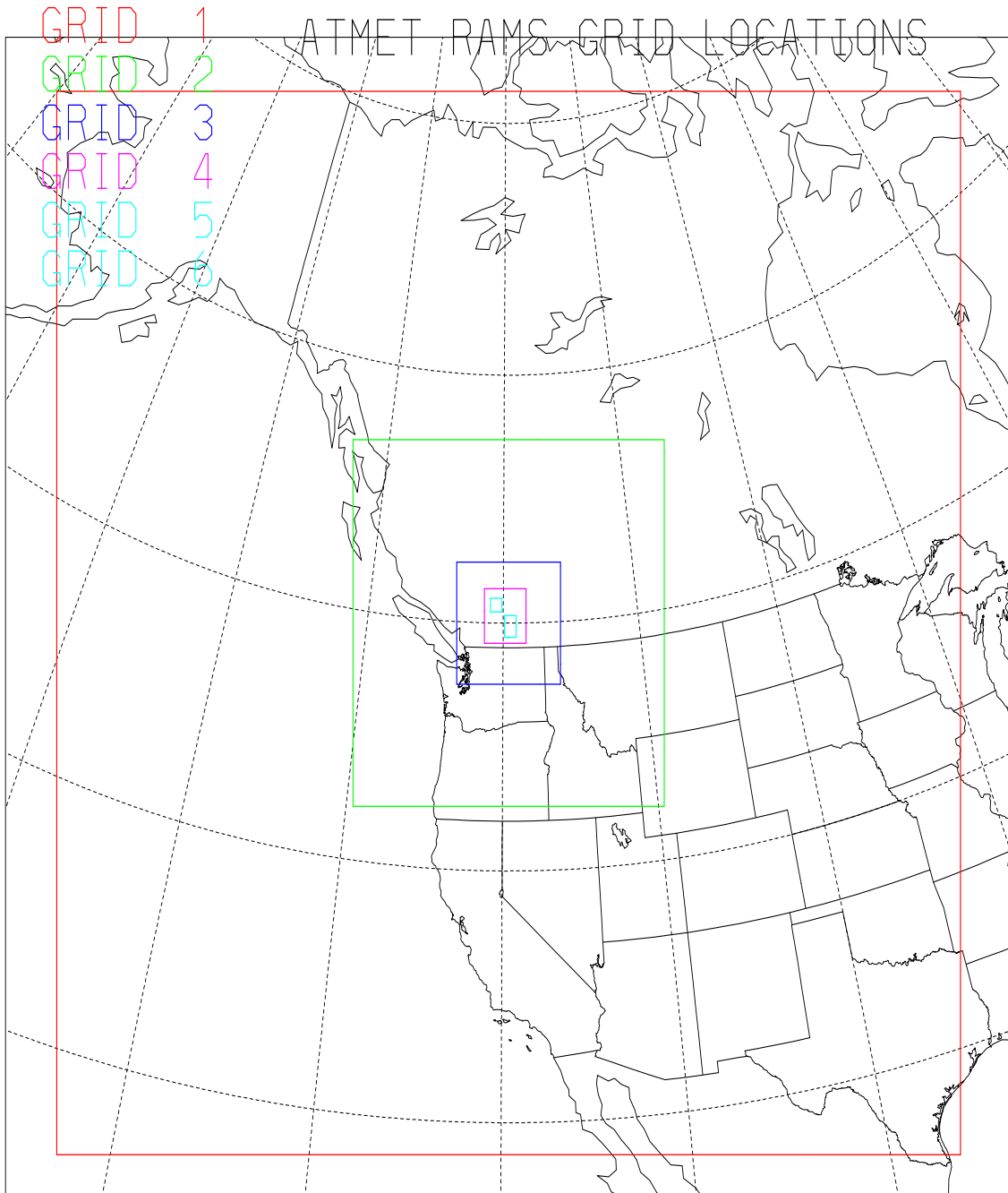


Figure 1: RAMS Modelling Domain.

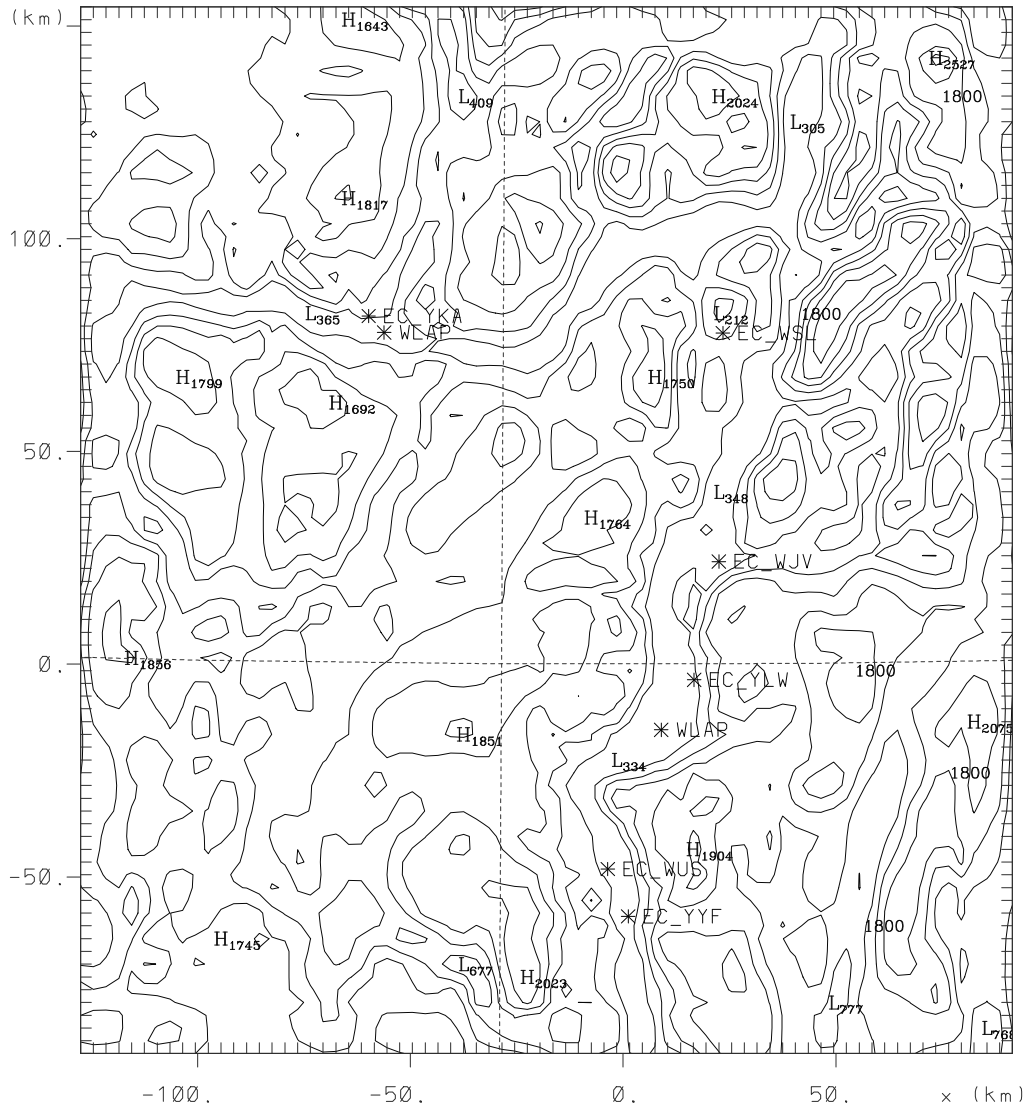


Figure 2: RAMS grid 4 (Thomson-Okanagan) at 3 km horizontal resolution. Topographical heights contoured in increments of 300 m.

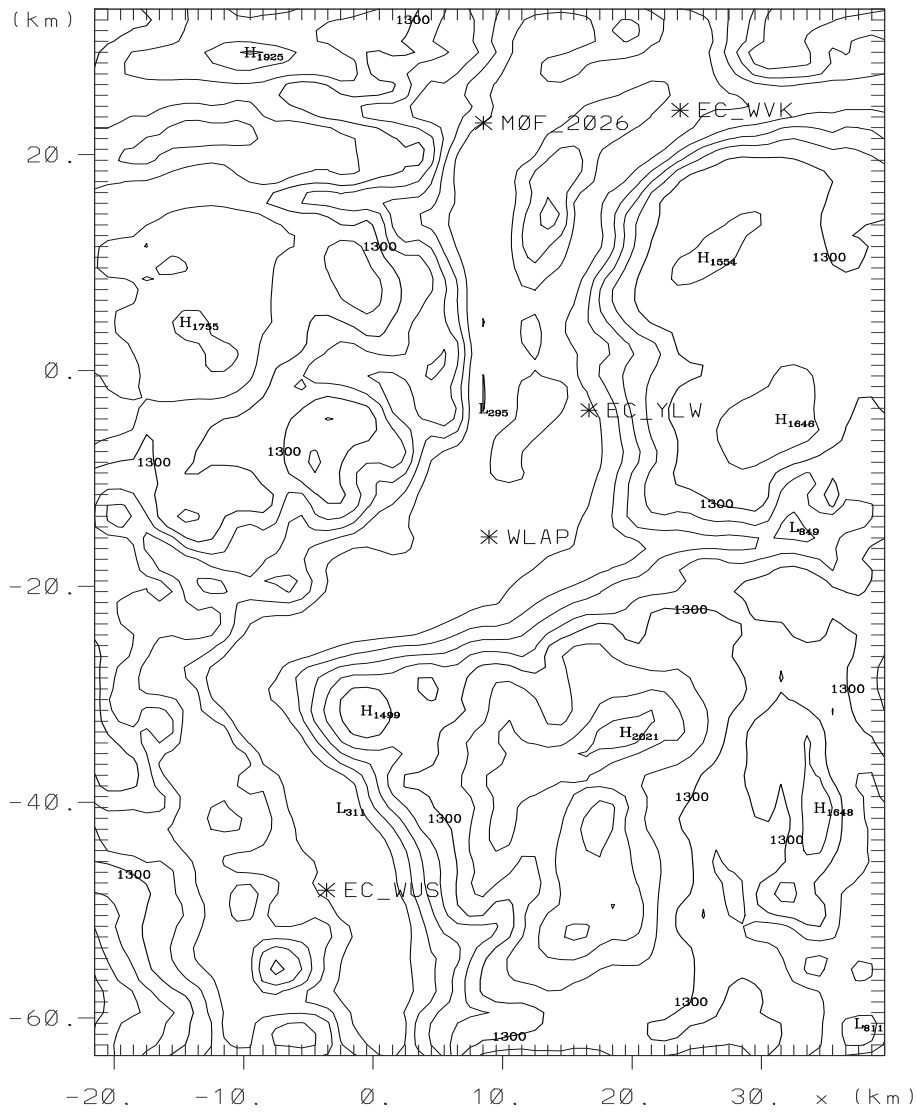


Figure 3: RAMS grid 5 (centered near Kelowna) at 1 km horizontal resolution. Topographical heights contoured in increments of 200 m.

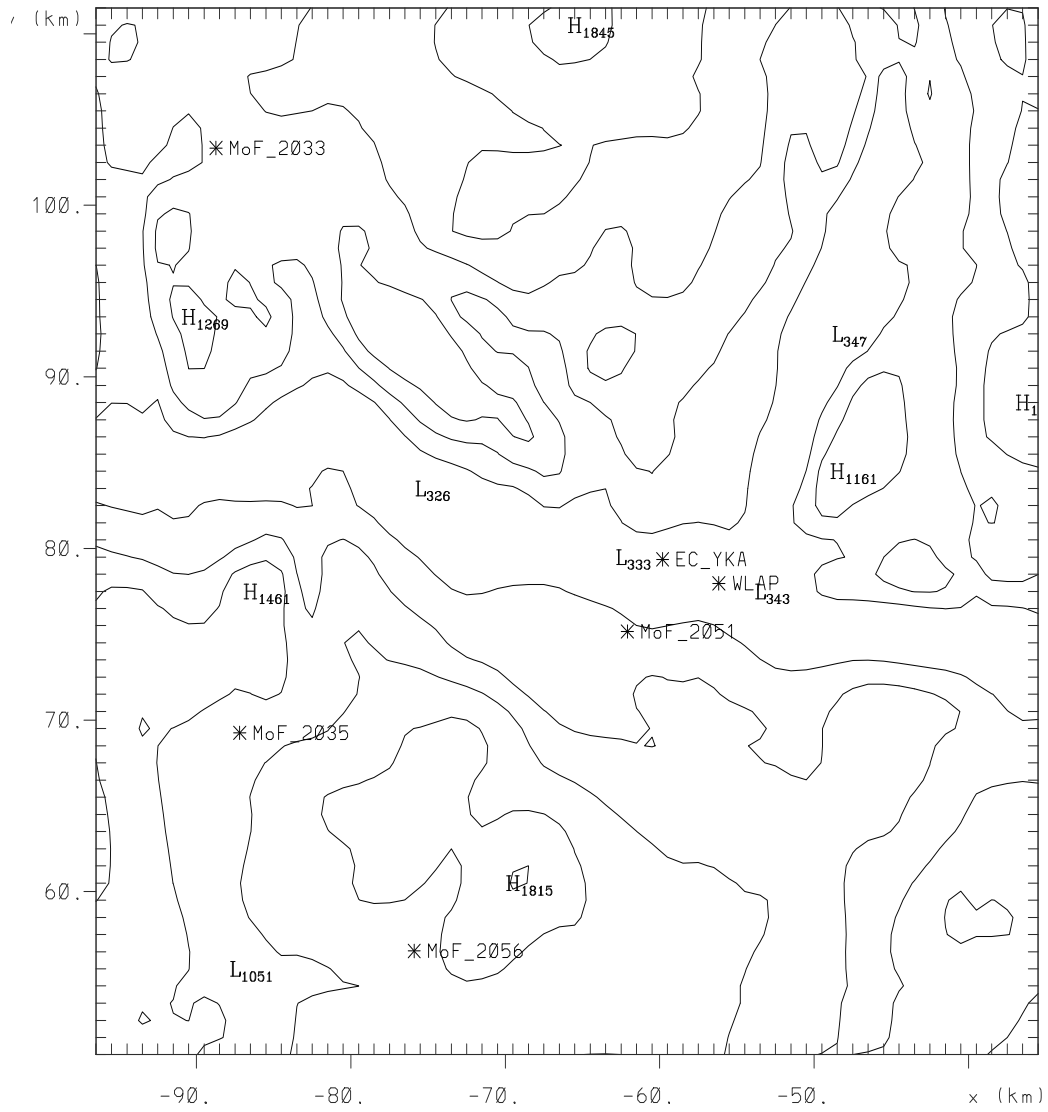


Figure 4: RAMS grid 6 (centered on Kamloops) at 1 km horizontal resolution. Topographical heights contoured in increments of 200 m.

2.2 Initialization and Nudging

Each modelling strategy was initialized and nudged using 90 km Eta fields alone; no local station data was utilized. FORECAST uses Eta forecast fields at three hour intervals. A new set of forecasts are produced every 24 hours; for modelling of any given day, the 0Z analysis of the next day is more desirable to use than the 24 hour forecast of the present day. Because of this, FORECAST was initialized at 0Z each day of the modelling period and set to run for 21 hours of simulation time. Each day was simulated in this manner. In contrast, HINDCAST was initialized at 0Z of the first day to be run continuously for the duration of the modelling period. On the occasion when this simulation had to be stopped (due to numerical instability, or a computer hardware problem), it was re-started 6 hours previous to the stop, and run continuously to the end of the period.

3 Validation

To assess the simulation skill of the two modelling strategies, a number of surface and upper air comparisons of modelled values with observed values were conducted. These comparisons included both statistical calculations and qualitative judgments. Comparisons done are a reflection of model validation strategies common in the literature. Significance testing for correlation coefficients was done by the B.C. Ministry of Water, Land and Air Protection and is shown in Appendix C. The WLAP analysis also presents a detailed categorization of simulation accuracy.

3.1 Inherent Difficulties

When comparing modelled parameters with observed parameters, several criteria must be noted. These are:

1. *Measurement Error.* Station observations cannot be considered error free. Assuming all meteorological stations were operating correctly, there are still errors inherent in the measuring equipment. Cup anemometers, used at Environment Canada (EC) and Ministry of Forests (MoF) sites, may have a wind speed error margin as high as 10% (Linacre, 1992)

and direction is reported to the nearest 10° for EC and just 45° for MoF. WLAP stations have a lower estimated error.

2. *Modelled vs. Observed Surface Fields.* Modelled values are instantaneous and represent a volume averaged value. Observed values are measured at a specific height, and are mean values over a specified period of time (e.g. hourly, 10min, 2min).
3. *Modelled vs. Observed Upper Air Soundings.* Sounding data is not an instantaneous snapshot of the vertical profile above a location. Sondes take well over an hour to ascend, and can drift horizontally a considerable distance in this time. Modelled soundings are an instantaneous profile of the grid cells above a point.
4. *Calm Periods.* Both the EC and MoF surface stations use anemometers that have a higher stall speed than those used by WLAP and the Ministry of Transportation (MoTH). During calm intervals, the EC and MoF stations can register zero wind values for a considerable portion of the time. In practice, any wind speed less than 1 m/s will register as zero at these stations.

Because of these criteria, a high quality simulation will always have some statistical error associated with it.

3.2 Validation Times and Locations

The RAMS model requires several hours of simulation time before its meteorological fields come into physical balance. This is referred to as ‘spin-up’ time. To account for spin-up, hourly validation of model output for the two modelling strategies began at 6Z each day and ended at 21Z. This allowed just one upper air validation time each day, occurring at 12Z (4 A.M. local time) at Kelowna YLW.

Surface validation of the 1 km resolution fields (grids 5 and 6) was performed using observations from surface meteorological stations (11 for the summer simulation and 9 for the winter simulation). Since RAMS grid 4, at 3 km resolution, also covers the entire area of interest in this study, its surface fields were also validated at several of the same station locations. In doing this, an indication of the difference in simulation skill at differing resolution is obtained. Statistical

comparisons of observed data to corresponding modelled values were done at individual surface station locations. Ensemble calculations were also done, using all station values together, to facilitate a direct comparison between the two modelling strategies. Modelled upper-air data were validated once a day at the EC YLW station.

The 11 surface stations used to validate the summer simulations are listed in table 2. Due to the fact that MoF stations are not maintained during the winter, fewer stations were available to validate the winter simulations. The late addition of three MoTH surface station datasets allowed a total of nine surface stations to be used to validate the winter simulations (see table 3).

Station Name	Grid	Symbol	Latitude	Longitude
Sparks Lake	6	MoF-2033	50.92	-120.87
Afton	6	MoF-2051	50.67	-119.48
Leighton Lake	6	MoF-2035	50.62	-120.84
Kamloops Brocklehurst	6	WLAP-1	50.70	-120.40
Kamloops A	6	EC-YKA	50.70	-120.45
Paska Lake	6	MoF-2056	50.50	-120.67
Vernon	5	EC-WJV	50.22	-119.27
Fintry	5	MoF-2026	50.21	-119.48
Kelowna College	5	WLAP-2	49.86	-119.48
Kelowna A	5	EC-YLW	49.97	-119.37
Summerland	5	EC-WUS	49.57	-119.65

Table 2: Surface stations used for summer validation

Station Name	Grid	Symbol	Latitude	Longitude
Kamloops Brocklehurst	6	WLAP-1	50.70	-120.40
Kamloops A	6	EC-YKA	50.70	-120.45
Wallopier	6	MoTH-21091	50.53	-120.48
Vernon	5	EC-WJV	50.22	-119.27
Kalamalka	5	MoTH-23097	50.21	-119.31
Kelowna College	5	WLAP-2	49.86	-119.48
Kelowna A	5	EC-YLW	49.97	-119.37
Summerland	5	EC-WUS	49.57	-119.65
McCulloch	5	MoTH-33099	50.76	-119.13

Table 3: Surface stations used for winter validation

3.3 Measures Used

The root mean square vector error (RMSVE) and the root mean square error (RMSE), are commonly used to evaluate model predictions (e.g. Willmott *et al*, 1985). The mean absolute difference (AD) and correlation coefficient (r), as described by Henmi (2000), were also used in this assessment. These measures are:

$$RMSVE = \left[\frac{\sum_{i=1}^n (u_{p,i} - u_{o,i})^2 + (v_{p,i} - v_{o,i})^2}{n} \right]^{\frac{1}{2}} \quad (1)$$

$$RMSE = \left[\frac{\sum_{i=1}^n (x_{p,i} - x_{o,i})^2}{n} \right]^{\frac{1}{2}} \quad (2)$$

$$AD = \frac{\sum_{i=1}^n |x_{p,i} - x_{o,i}|}{n} \quad (3)$$

$$r = \frac{\sum_{i=1}^n x_{p,i} * x_{o,i}}{\left(\sum_{i=1}^n y_{p,i}^2 * \sum_{i=1}^n y_{o,i}^2 \right)^{\frac{1}{2}}} \quad \text{with } y_{p,i} = x_{p,i} - \bar{x}_p \quad (4)$$

where u and v are the east-west and north-south vector wind components, x is any scalar quantity, n is the total number of paired data values (one observed, one modelled) and the subscripts p and o denote predicted and observed values respectively. A lower value for both RMSE and AD indicate better model performance. Correlation (r) is a measure of the degree of linear relationship between two variables and can be assessed for significance using a standard F test. A value of +1.0 indicates perfect positive correlation and -1.0 as perfect negative correlation. RMSE, AD, and r were determined for surface level wind and temperature at each surface station location; ‘n’ is the number of hourly observations used at a station location for a station specific statistic, and represents the total number of observations at all times and locations when calculating an ensemble statistic.

Upper air validation was done at the Kelowna YLW location. 10 different modelled levels were chosen, spaced throughout the lowest 2 km of the atmosphere. Each level was matched to the

closest level from a high resolution sounding. Data is recorded in these soundings every 10 s, which typically corresponds to a step of roughly 50 m in height. Because of this, the error in matching a model level with a sounding level is a maximum of approximately 25 m, which was considered reasonable. In the majority of cases, the error in vertical level matching was much lower than this amount, and always is identical for both modelling strategies. On these levels, RMSVE was determined for wind vector, and RMSE for temperature, dew-point temperature and pressure.

4 Results

4.1 Modelling Experiences

There was little difficulty experienced in RAMS' modelling of the summer period for both strategies. On a few occasions, the model became numerically unstable and stopped. This is not an uncommon experience in mesoscale modelling and usually is fixed by restarting the model with a shorter time-step. This was done successfully on these occasions.

Difficulties were encountered during the modelling of the winter period that could not be as easily resolved. There were several days within the two-week interval that RAMS could not simulate using the configuration chosen for this study. For these days, both simulations became numerically unstable and stopped, regardless of the time-step chosen. It was determined that RAMS was having difficulty with the simulations on grid 1 only; when this grid was excluded from the domain (ie using 5 nested grids instead of 6) there was no instability. Because of this, modelling of the winter period was conducted using 5 nested grids, with the largest horizontal grid spacing being 27 km. Figure 1 verifies that the 27 km grid is large enough to capture significant features of the synoptic flow; therefore using 5 nested grids instead of 6 likely does not lead to lower-quality simulations.

4.2 Computer requirements

Model cpu time required for each simulation time-step varied not only with number of processors used, as would be expected, but also by day and hour of day. In general, modelling through

evening hours progressed faster than daytime hours, and modelling of an overcast day faster than a clear day. It is likely that the radiation and convection schemes used within the RAMS model in this study were demanding on computer time. This is supported by observations in the RAMS manual (Walko and Tremback, 2002). Choice of simpler parameterizations are possible, which would result in shorter simulation times. Whether or not this would reduce the quality of the simulated fields, and by what factor, is difficult to estimate.

RAMS simulations used either 10 or 12 processors of the 28-processor SGI Origin 3400.

Typically, two simulations were running at the same time, which used a large portion of the computers capacity. Due to differences in the individual days as outlined above, simulating one day with RAMS required between one-half to one day of computer cpu time. There was not an appreciable time difference between modelling strategies. Modelling of both summer and winter periods experienced similar time requirements.

RAMS, like other mesoscale models, calculates and stores many atmospheric variables during a simulation. Having the model write analysis files every hour can amount to huge data storage requirements. Currently, there is an option to have the model write 'lite' analysis files that contain a smaller subgroup (of the operator's choice) of variables. This option was chosen for the simulations, which required approximately 6 Mb of storage space per gridded field, per hour. Six grids were used in the modelling (summer period), so roughly 36 Mb of storage was needed for each simulated hour, for each modelling strategy. In the near future, the RAMS user will also be able select what gridded levels appear in the lite analysis files. Currently, all levels are written.

4.3 Surface Validation

4.3.1 Statistical Validation

Tables 4 and 5 show mean wind speed and the standard deviation in wind speed for observations and simulations at the surface stations used for validating the 1 km fields. At a station location, there was usually greater variation in observed wind speed than either simulation produced. For a few stations, higher simulated mean wind speeds over observations are a result of high anemometer threshold. For most locations, HINDCAST produced lower mean wind speeds than FORECAST, coupled with smaller standard deviations. As can be expected for a region of

complex terrain, there was considerable variability between surface station locations for both observed and modelled winds.

STATION	OBSERVED		HINDCAST		FORECAST	
	Mean Speed (m/s)	Std Deviation (m/s)	Mean Speed (m/s)	Std Deviation (m/s)	Mean Speed (m/s)	Std Deviation (m/s)
MoF-2033	0.31	0.49	1.62	0.70	1.80	0.97
MoF-2051	2.20	1.32	2.27	1.20	2.44	1.22
MoF-2035	1.23	1.35	1.26	0.86	1.55	1.01
WLAP-Kamloops	2.15	1.29	1.33	0.64	1.57	1.05
EC-YKA	1.15	1.53	1.68	0.59	1.84	0.79
MoF-2056	1.53	1.28	1.71	0.89	1.84	0.94
EC-WJV	1.87	1.30	1.57	0.95	1.96	1.00
MoF-2026	1.04	1.07	2.06	1.24	2.03	1.24
WLAP-Kelowna	2.24	1.14	1.23	0.58	1.41	0.85
EC-YLW	1.12	1.23	1.57	0.83	1.73	1.09
EC-WUS	2.36	0.82	1.74	1.02	1.94	1.41

Table 4: Observed and Modelled Winds at Surface Station Locations (Summer Simulation, 1km resolution)

STATION	OBSERVED		HINDCAST		FORECAST	
	Mean Speed (m/s)	Std Deviation (m/s)	Mean Speed (m/s)	Std Deviation (m/s)	Mean Speed (m/s)	Std Deviation (m/s)
WLAP-Kamloops	1.08	1.21	1.22	0.74	1.28	0.73
EC-YKA	1.98	0.96	1.58	0.69	2.57	2.41
MoTH-2109	0.57	0.65	1.37	0.71	1.51	0.85
EC-WJV	2.24	1.40	1.75	0.91	1.55	1.13
MoTH-23097	1.31	0.95	1.30	0.77	1.67	0.89
WLAP-Kelowna	2.07	1.60	2.17	1.37	2.50	1.52
EC-YLW	1.18	0.97	1.46	0.70	1.45	0.84
EC-WUS	1.32	0.95	1.31	0.77	1.38	1.00
MoTH-33099	1.83	1.11	1.46	0.41	1.34	0.53

Table 5: Observed and Modelled Winds at Surface Station Locations (Winter Simulation, 1km resolution)

Statistical assessments in Tables 6 and 7 suggest that the two modelling strategies had variable success at predicting surface station observations. For most station locations, HINDCAST and FORECAST behaved similarly; each tended to predict well at the same stations and conversely have difficulty at the same locations. During both simulation periods, the correlation coefficients

for wind components and wind speed were low at half or more stations. Although this could be due to poor model performance, there are other possibilities as well. In particular, model timing of a synoptic pattern can have a great impact on validation statistics; RAMS can model a feature of the local wind flow before or after it actually occurs. A surface station location also may not be representative of the surrounding area. A RAMS surface wind vector is a volume average for a 1 km² slab that is 25m thick. This is being compared to a spot measurement where local influences, that may not be resolved within RAMS, may have a strong effect on the wind. Although windrose diagrams (presented in Appendix B) can be used to assess the first statement to some degree, addressing the second statement is beyond the scope of this study.

Tables 8 and 9 present validation results for the 3 km fields using all the EC and WLAP surface stations within this domain. This was done to contrast simulation quality at differing model resolution. On this grid, each cell represents a much greater volume of the atmosphere than for the 1 km grids, so it was expected that agreement would be lower in general. Although this was evident with HINDCAST fields, FORECAST fields did not show this feature. For both simulations, there was very little difference in wind speed error when comparing 3 km resolution to 1 km. This indicates that (for HINDCAST) it is primarily modelled wind direction that benefits from smaller grid spacings.

Tables 10 and 11 present ensemble validation results using all station locations and times for the 1 km fields. Error in wind direction is also included here. Clearly HINDCAST produces surface wind fields that are a better match to observations, but improvement over FORECAST fields is not large. Significance testing at the 95 % confidence interval was done on individual and ensemble correlations. Tables 2 and 4 in Appendix A show in most cases the small differences between HINDCAST and FORECAST correlations are not significant. At no station does one simulation have a significantly higher temperature correlation than the other. During the winter simulation, the HINDCAST ensemble correlation for the u component of wind is significantly higher than for FORECAST. This is the only ensemble correlation value that is significantly different for the two modelling strategies.

HINDCAST								
STATION	n	CORRELATION COEFFICIENT				ROOT MEAN SQUARE ERROR		
		u	v	T	Speed	Wind Vector	T	Speed
MoF-2033	205	0.09	0.43	0.91	0.51	1.64	2.76	1.45
MoF-2051	205	0.54	0.66	0.92	0.24	2.44	2.21	1.56
MoF-2035	205	0.20	0.54	0.920	0.61	1.61	2.87	1.07
WLAP-1	203	-0.08	-0.11	0.89	0.28	3.09	2.66	1.52
EC-YKA	204	0.16	0.02	0.85	0.05	2.48	2.98	1.69
MoF-2056	205	0.62	0.57	0.94	0.62	1.64	1.84	1.02
EC-WJV	204	0.28	-0.05	0.90	-0.06	2.87	2.78	1.69
MoF-2026	205	0.50	0.45	0.90	0.21	2.37	2.33	1.78
WLAP-2	204	0.42	0.39	0.89	0.11	2.34	3.19	1.59
EC-YLW	205	0.19	0.14	0.86	0.05	2.26	3.29	1.52
EC-WUS	205	0.35	-0.04	0.86	-0.22	2.67	2.52	1.58
FORECAST								
STATION	n	CORRELATION COEFFICIENT				ROOT MEAN SQUARE ERROR		
		u	v	T	Speed	Wind Vector	T	Speed
MoF-2033	205	-0.03	0.29	0.88	0.53	1.99	3.16	1.69
MoF-2051	205	0.43	0.64	0.94	0.17	2.61	1.85	1.66
MoF-2035	205	0.29	0.49	0.91	0.62	1.75	3.16	1.12
WLAP-1	203	0.05	-0.02	0.90	0.31	3.10	2.75	1.51
EC-YKA	204	0.03	0.07	0.87	0.13	2.73	2.95	1.77
MoF-2056	205	0.51	0.56	0.94	0.60	1.80	1.84	1.09
EC-WJV	204	0.50	0.15	0.92	-0.13	2.80	3.00	1.74
MoF-2026	205	0.38	0.04	0.89	0.19	2.62	2.73	1.78
WLAP-2	204	0.32	0.31	0.92	0.14	2.52	2.09	1.56
EC-YLW	205	0.15	-0.10	0.87	0.12	2.63	3.74	1.66
EC-WUS	205	0.21	0.14	0.89	-0.24	3.01	2.38	1.85

Table 6: Modelling Validation at Surface Station Locations (Summer Simulation, 1km resolution)

HINDCAST								
STATION	n	CORRELATION COEFFICIENT				ROOT MEAN SQUARE ERROR		
		u	v	T	Speed	Wind Vector	T	Speed
WLAP-1	222	0.36	-0.08	0.80	0.13	2.63	2.3	1.65
EC-YKA	224	0.17	-0.05	0.76	0.10	1.98	2.57	1.57
MoTH-33099	223	0.31	0.84	0.78	0.64	1.89	2.81	1.29
EC-WJV	222	0.24	0.06	0.74	0.12	2.2	2.78	1.16
MoTH-23097	223	0.31	0.2	0.77	0.17	2.1	2.26	1.12
WLAP-2	224	0.23	0.24	0.66	0.05	2.39	2.93	1.23
EC-YLW	224	-0.45	0.33	0.72	0.40	2.16	2.58	1.15
EC-WUS	224	0.27	-0.16	0.72	0.19	2.33	2.89	1.15
MoTH-21091	223	-0.12	0.76	0.75	0.60	1.34	3.71	1.01
FORECAST								
STATION	n	CORRELATION COEFFICIENT				ROOT MEAN SQUARE ERROR		
		u	v	T	Speed	Wind Vector	T	Speed
WLAP-1	222	0.24	-0.05	0.76	0.26	2.82	2.52	1.71
EC-YKA	224	0.07	-0.03	0.72	0.11	2.08	2.77	1.59
MoTH-33099	223	0.31	0.89	0.82	0.76	1.76	2.72	1.18
EC-WJV	222	0.17	0.20	0.71	0.09	2.23	2.9	1.25
MoTH-23097	223	0.16	0.15	0.77	0.26	2.32	2.33	1.19
WLAP-2	224	0.04	0.08	0.65	-0.09	2.47	2.98	1.36
EC-YLW	224	-0.35	0.27	0.69	0.41	2.23	2.72	1.15
EC-WUS	224	0.31	0.04	0.72	-0.06	3.63	2.92	2.71
MoTH-21091	223	-0.08	0.79	0.76	0.49	1.48	3.79	1.22

Table 7: Modelling Validation at Surface Station Locations (Winter Simulation, 1km resolution)

HINDCAST								
STATION	n	CORRELATION COEFFICIENT				ROOT MEAN SQUARE ERROR		
		u	v	T	Speed	Wind Vector	T	Speed
WLAP-1	203	-0.15	-0.12	0.89	0.07	3.10	2.75	1.57
EC-YKA	204	0.08	0.05	0.86	0.02	2.70	2.63	1.84
EC-WJV	204	0.22	-0.07	0.91	-0.10	2.78	3.10	1.69
WLAP-2	204	0.37	0.28	0.88	0.07	2.46	3.25	1.62
EC-YLW	205	0.05	0.35	0.82	0.00	2.73	3.33	1.93
EC-WUS	205	0.33	-0.10	0.86	-0.10	2.72	2.61	1.52
FORECAST								
STATION	n	CORRELATION COEFFICIENT				ROOT MEAN SQUARE ERROR		
		u	v	T	Speed	Wind Vector	T	Speed
WLAP-1	203	0.10	0.17	0.90	0.19	2.91	2.96	1.56
EC-YKA	204	0.12	0.06	0.87	0.20	2.82	2.39	1.90
EC-WJV	204	0.39	0.28	0.92	-0.05	2.77	3.47	1.72
WLAP-2	204	0.29	0.22	0.92	0.12	2.63	2.07	1.67
EC-YLW	205	0.06	0.07	0.85	0.07	3.21	3.02	2.19
EC-WUS	205	0.15	0.16	0.89	-0.13	2.97	2.19	1.77

Table 8: Modelling Validation at Surface Station Locations (Summer Simulation, 3km resolution)

HINDCAST								
STATION	n	CORRELATION COEFFICIENT				ROOT MEAN SQUARE ERROR		
		u	v	T	Speed	Wind Vector	T	Speed
WLAP-1	222	0.11	-0.11	0.80	0.09	2.93	2.36	1.59
EC-YKA	224	0.12	-0.05	0.77	0.11	1.98	1.99	1.49
EC-WJV	222	0.16	0.08	0.74	0.17	1.95	3.06	1.08
WLAP-2	224	0.23	0.14	0.66	0.03	2.36	2.83	1.26
EC-YLW	224	-0.26	0.33	0.75	0.04	2.37	2.57	1.52
EC-WUS	224	0.19	-0.10	0.73	0.22	2.33	2.46	1.22
FORECAST								
STATION	n	CORRELATION COEFFICIENT				ROOT MEAN SQUARE ERROR		
		u	v	T	Speed	Wind Vector	T	Speed
WLAP-1	222	0.20	-0.01	0.78	0.14	2.94	2.46	1.65
EC-YKA	224	0.05	-0.02	0.72	0.11	2.13	2.20	1.60
EC-WJV	222	0.14	0.13	0.71	0.18	1.96	3.17	1.10
WLAP-2	224	0.07	0.02	0.66	-0.10	2.44	2.86	1.40
EC-YLW	224	-0.11	0.18	0.72	0.11	2.45	2.60	1.55
EC-WUS	224	0.29	0.08	0.72	0.02	2.98	2.51	1.88

Table 9: Modelling Validation at Surface Station Locations (Winter Simulation, 3km resolution)

Root Mean Square Error					
STRATEGY	Wind Vector (m/s)		T (°C)	Wind Speed (m/s)	Wind Dir. (deg.)
HINDCAST	2.36		2.71	1.52	92.6
FORECAST	2.55		2.77	1.61	93.2
Absolute Difference					
STRATEGY	u (m/s)	v (m/s)	T (°C)	Wind Speed (m/s)	Wind Dir. (deg.)
HINDCAST	1.37	1.18	2.16	1.20	75.1
FORECAST	1.53	1.21	2.20	1.27	76.1
Correlation Coefficient					
STRATEGY	u	v	T	Wind Speed	
HINDCAST	0.22	0.36	0.89	0.16	
FORECAST	0.21	0.32	0.90	0.17	

Table 10: Ensemble Validation at 1 km resolution (Summer Period), n = 2010

Root Mean Square Error					
STRATEGY	Wind Vector (m/s)		T (°C)	Wind Speed (m/s)	Wind Dir. (deg.)
HINDCAST	2.14		2.75	1.28	91.5
FORECAST	2.41		2.88	1.56	95.0
Absolute Difference					
STRATEGY	u (m/s)	v (m/s)	T (°C)	Wind Speed (m/s)	Wind Dir. (deg.)
HINDCAST	1.19	1.10	2.24	1.00	73.3
FORECAST	1.37	1.11	2.31	1.13	77.3
Correlation Coefficient					
STRATEGY	u	v	T	Wind Speed	
HINDCAST	0.24	0.42	0.76	0.33	
FORECAST	0.17	0.44	0.74	0.28	

Table 11: Ensemble Validation at 1 km resolution (Winter Period), n = 2251

Wind RMSE by simulation hour for the ensemble was plotted for both simulations (Figures 5 and 6). The values plotted are simple averages of each hourly RMSE calculation of each modelled day. The summer time-series shows that error increases dramatically near the end of a modelled day for FORECAST and that this is the only portion of the day when HINDCAST appears to have an advantage. One reason for this may be that the ETA forecast fields used for nudging

possess greater error themselves later in the day. However, this feature was not evident in the winter time-series; during this period simulation error is relatively uniform throughout the day.

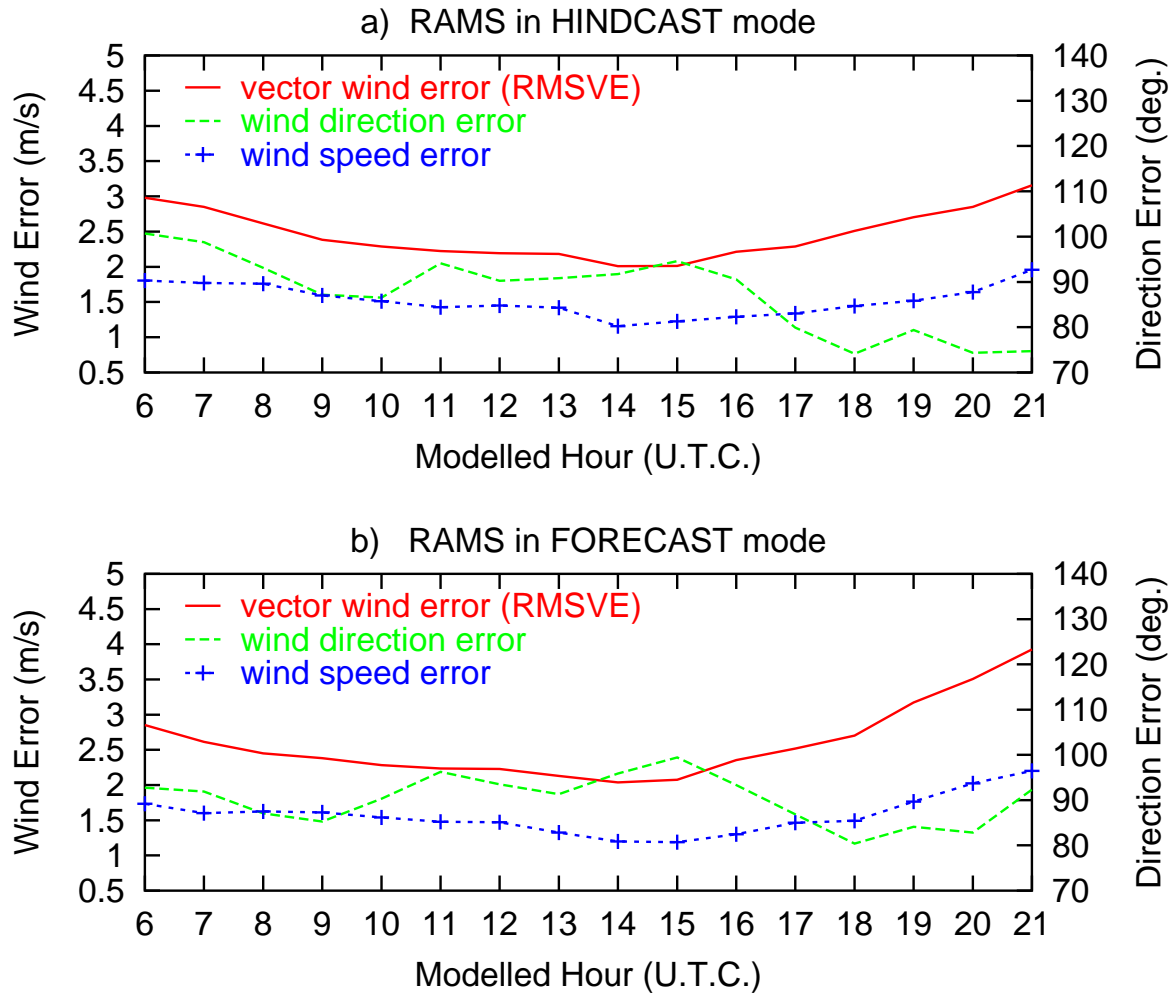


Figure 5: Wind RMSE by hour of simulation for RAMS in a) HINDCAST mode, and b) FORECAST mode (summer simulation, 1km resolution).

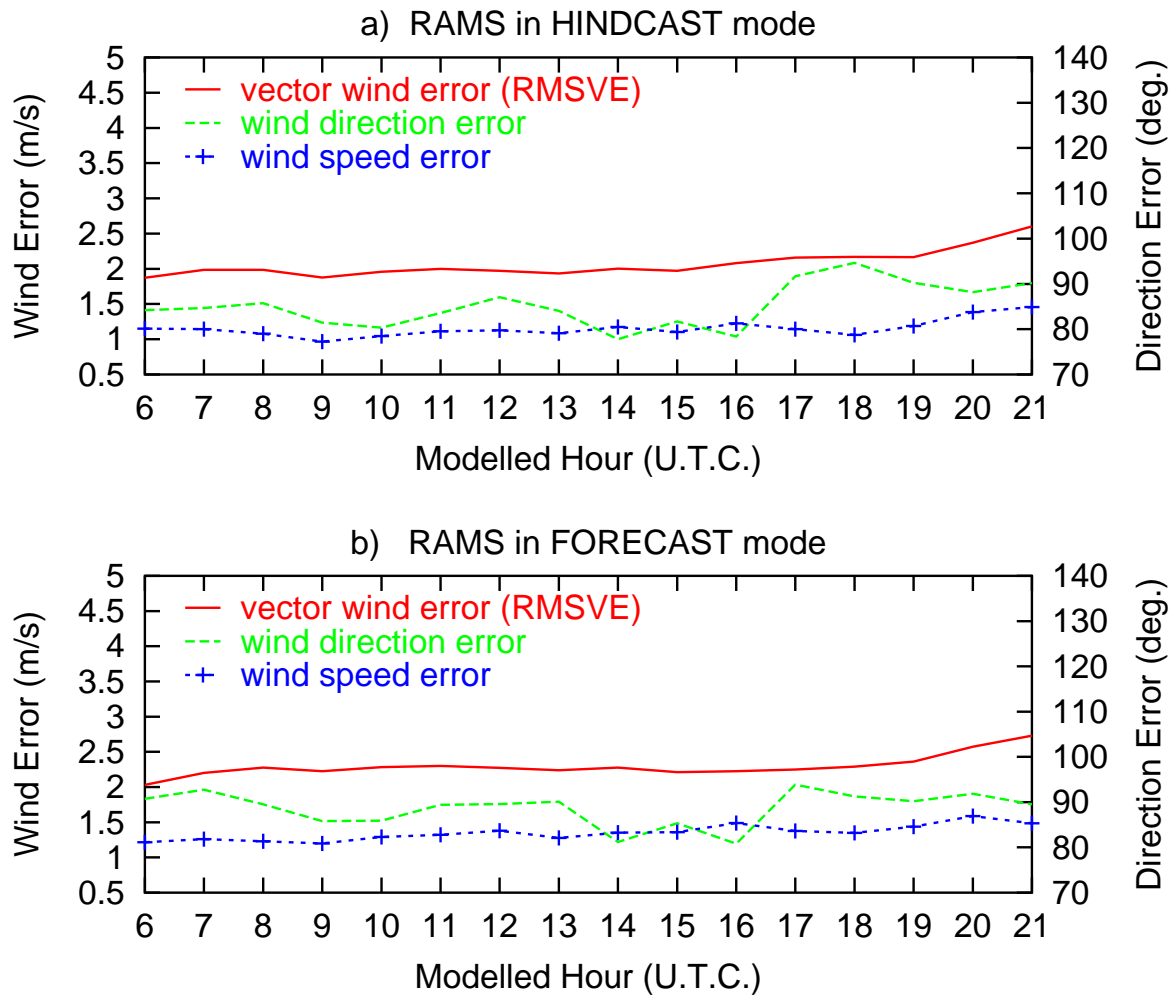


Figure 6: Wind RMSE by hour of simulation for RAMS in a) HINDCAST mode, and b) FORECAST mode (winter simulation, 1km resolution).

4.3.2 Qualitative Validation

HINDCAST wind field plots, with observed station winds, are presented in figures 7 through 10 to show how simulated surface winds appear during periods of relatively good agreement (Figures 7 and 8) and poor agreement (Figures 9 and 10). All 4 plots outline the complexity of wind patterns in the Thomson-Okanagan area. It is evident that RAMS' placing of surface convergence or divergence zones can have great impact on agreement with some surface station locations. FORECAST plots have similar characteristics and are not shown here.

"20Z June 20 Grid 5"

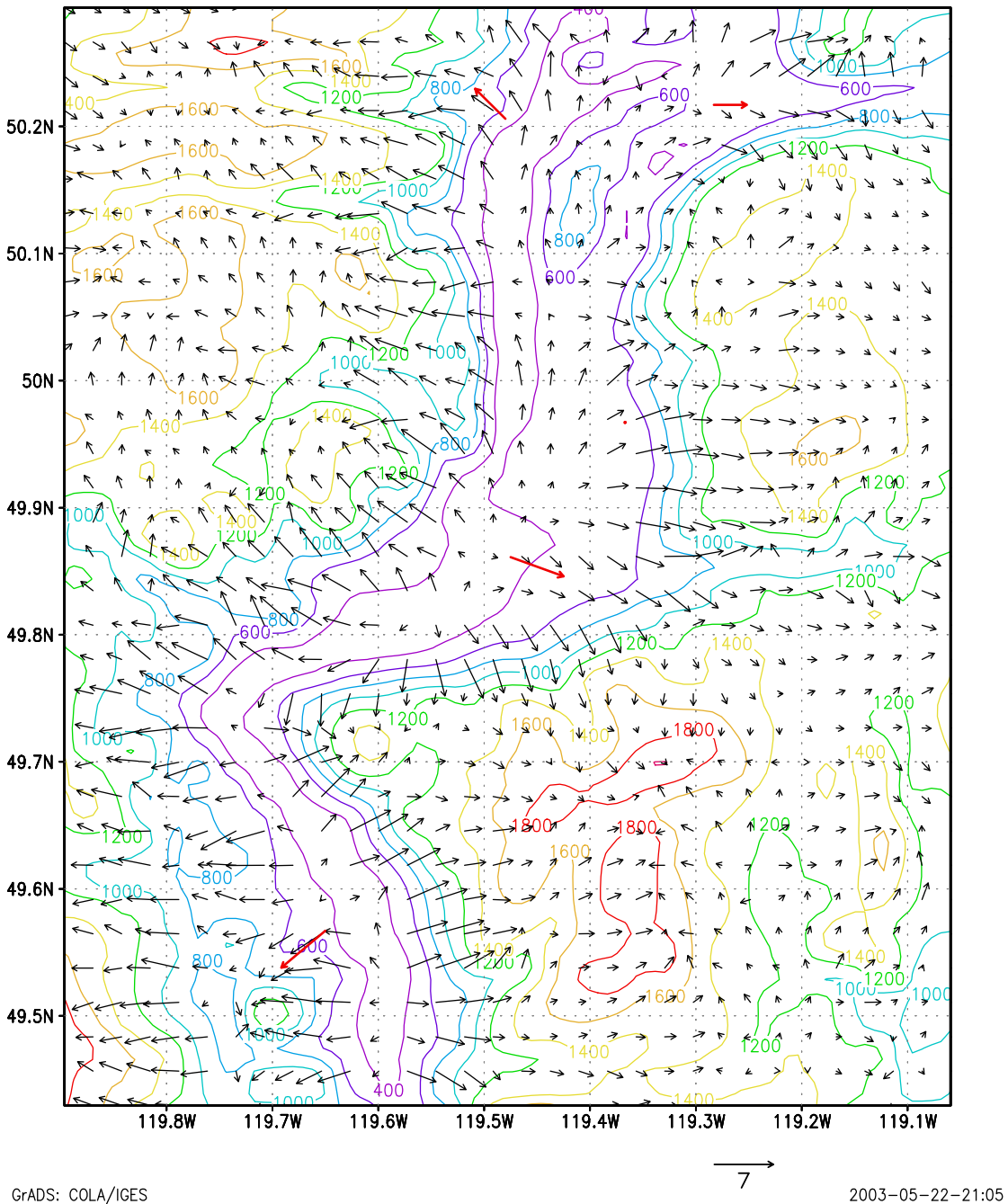
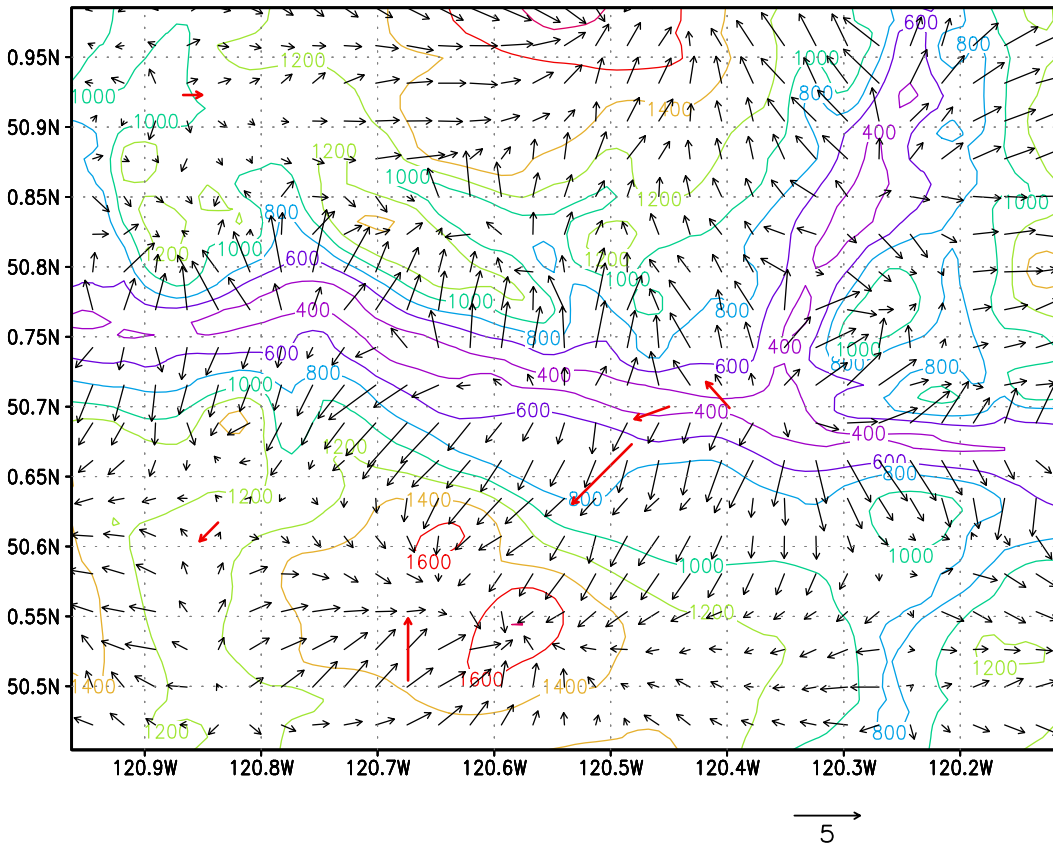


Figure 7: HINDCAST modelled winds with observed wind vectors in red. Example of 'good' agreement on grid 5 during summer simulation

"18Z June 20 Grid 6"

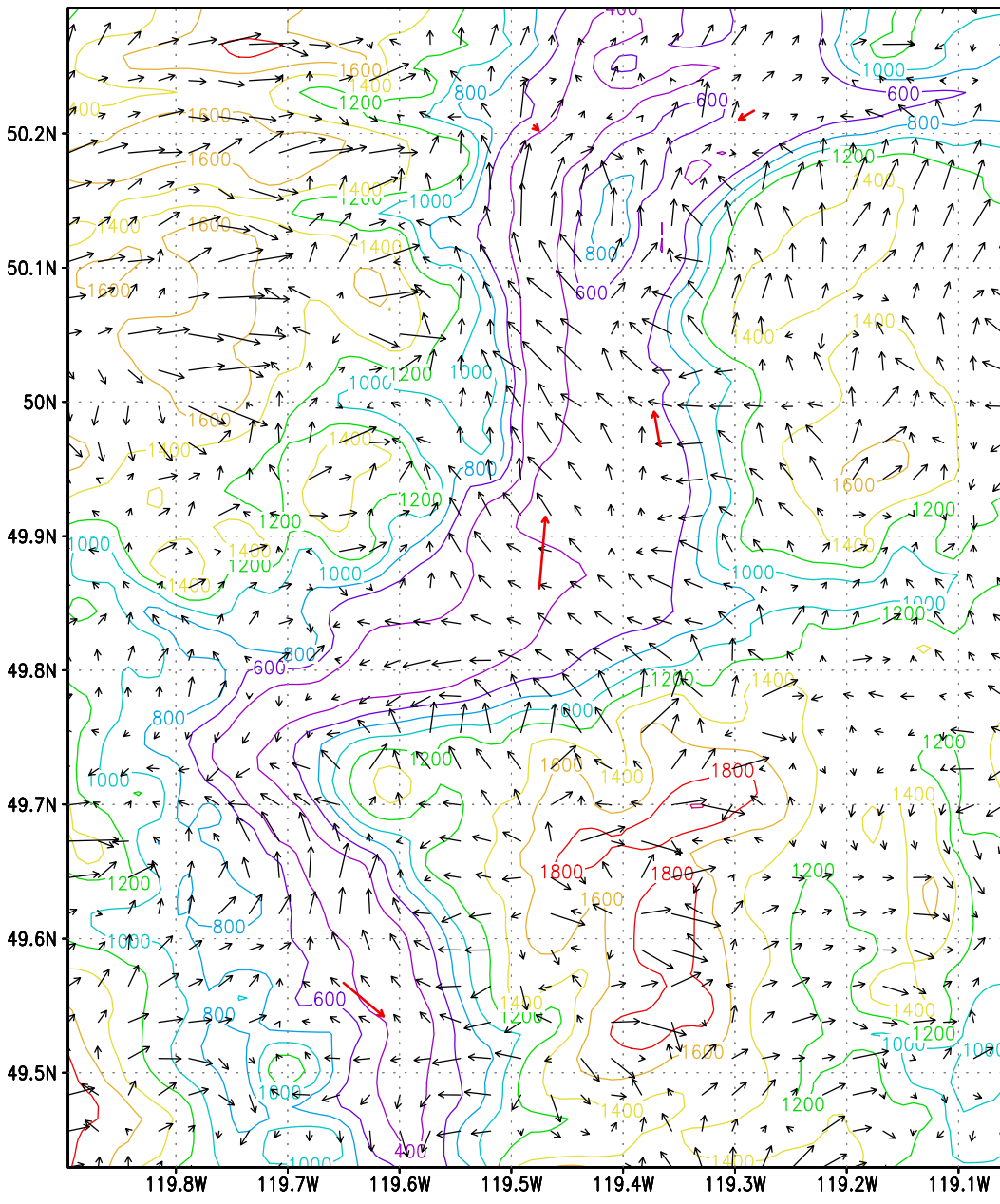


GrADS: COLA/IGES

2003-05-22-21:12

Figure 8: HINDCAST modelled winds with observed wind vectors in red. Example of 'good' agreement on grid 6 during summer simulation

"12Z June 17 Grid 5"



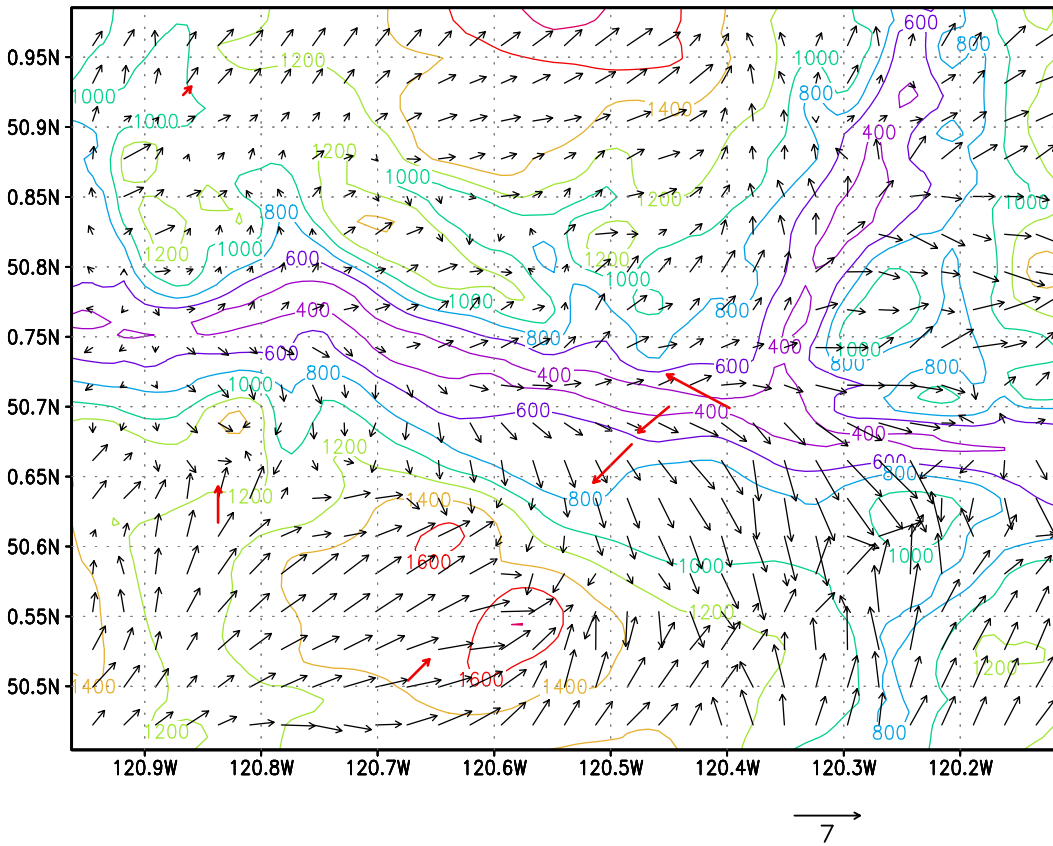
GrADS: COLA/IGES

→
5

2003-05-22-21:39

Figure 9: HINDCAST modelled winds with observed wind vectors in red. Example of 'poor' agreement on grid 5 during summer simulation

"18Z June 17 Grid 6"



GrADS: COLA/IGES

2003-05-22-21:42

Figure 10: HINDCAST modelled winds with observed wind vectors in red. Example of 'poor' agreement in grid 6 during summer simulation

Observing time sequences of modelled and observed station wind vectors (not included in this report) revealed that at several station locations RAMS captured a major shift in observed wind direction, but not at the hour at which it was observed. It is not uncommon for the modelled timing of systems in a prognostic model to be different than observed (e.g. McQueen *et al*, 1995). Although RAMS may resolve local circulations well, a modelled feature could occur at a different hour than when it occurred in real time. This effect has an impact on wind error calculations, and likely has a large impact on model correlations.

To gain an understanding of what influence modelled timing had on statistical comparisons, windrose diagrams were constructed for several surface stations. Four surface station locations (two during the summer and two during the winter) were chosen that had relatively good statistical agreement with observations, and windrose diagrams were constructed for HINDCAST, FORECAST and observations for each. Conversely, four locations of relatively poor statistical agreement were also chosen (see Appendix B). A note of caution is required before viewing these figures: frequency percentiles that show the portion of time wind flow was from a specific direction are scaled to each windrose diagram separately. These frequency rings can have different magnitudes from one diagram to the next.

Figure 13 shows that the dominant southerly flow experienced at MOF-2035 during the summer period was captured well by both simulations but the modelled westerly flow was not as good a match (especially for HINDCAST). This corresponds or ‘makes sense’ when compared to the earlier statistical parameters from Table 6: the u wind component (E-W) correlation was lower (0.2 and 0.29 for HINDCAST and FORECAST respectively) than the v wind (N-S) component (0.54, 0.49). Since MOF stations report wind direction to the nearest 45 °, agreement at this station should be considered quite good.

Figure 15 (station MoTH-21091 during winter) shows a station location that experienced a prominent bi-directional flow for the two-week period. Both simulations captured the dominant N-S component of the distribution, but had more variability with the E-W component than observed. The high frequency of southerly flow was biased 20° west by both HINDCAST and FORECAST. This corresponds to a high v correlation (0.76, 0.79) and a very poor u correlation (-0.12, -0.08). RMSVE (1.34, 1.48) was the lowest for all stations during the winter simulations. Figure 17 presents an example of a station location (WLAP-1) where simulations have both poor

statistical agreement and windrose diagrams that are not a good representation of observations. RAMS clearly did not produce surface winds that matched observations at this location during the summer simulations. The poor RMSVE and correlation values were a good indication of simulation skill in this case. Figure 18 is another example of qualitatively poor agreement. Although high RMSVE values support this, correlation values for FORECAST (0.5, 0.15) indicate that agreement was reasonably good. For this case, correlation coefficient was not a good indicator of model performance.

Figure 19 represents a situation where both u and v correlations and RMSVE indicate poor model performance for both simulations, but the windrose diagrams indicate that agreement was good. The dominant East/South-East flow was captured by both simulations at this location (WLAP-1 in winter). It is likely that much of the statistical error for the modelled winds at this location is due to model timing.

Figure 20, the last 'poor' example, shows observed and modelled circulation at WLAP-2 during the winter period. Clearly the poor statistical values result from the simulations not capturing the South-Westerly flow experienced at this station.

4.4 Upper Air Validation

Upper air validation is presented in tables 12 and 13. Again the HINDCAST strategy achieved better wind agreement by a small margin. Although error in dew-point temperatures were similar for the two summer simulations, error for temperature was considerably higher for HINDCAST. This was not evident for the winter simulations, when temperature RMSE values were similar. RAMS' performance in predicting upper air temperature varied significantly for both modelling strategies. Modelled and observed soundings were plotted to gain a better understanding of when the model was having difficulty. These plots showed that error in modelling temperature (but not necessarily dew-point temperature) increased during evenings of high stability. The difficulty a mesoscale model can have in predicting boundary layer features (particularly temperature profiles) has been documented in the past (e.g. Lyons *et al*, 1995). RAMS tended to under-predict, and on one occasion miss altogether, surface based inversions. Temperature agreement during evenings that did not develop strong stability was typically quite good. As an

indication of this behaviour for the summer simulations, Figure 11 has modelled and observed temperature profiles for an evening without strong stability and the particular evening when both models failed to capture the strong surface inversion observed. The winter period did not have evenings with strong stability. Figure 12 has modelled and observed temperature profiles for an evening of relatively good agreement and relatively poor agreement.

MODEL	RMSE (wind vector) m/s	RMSE (T) °C	RMSE (T _d) °C	RMSE (P) hPa
6HOUR	2.66	2.84	2.99	2.32
3HOUR	2.80	1.89	2.87	2.18

Table 12: Upper Air Validation using YLW upper air data (Summer Period)

MODEL	RMSE (wind vector) m/s	RMSE (T) °C	RMSE (T _d) °C	RMSE (P) hPa
6HOUR	2.90	2.11	1.63	2.64
3HOUR	3.18	2.04	2.01	3.45

Table 13: Upper Air Validation using YLW upper air data (Winter Period)

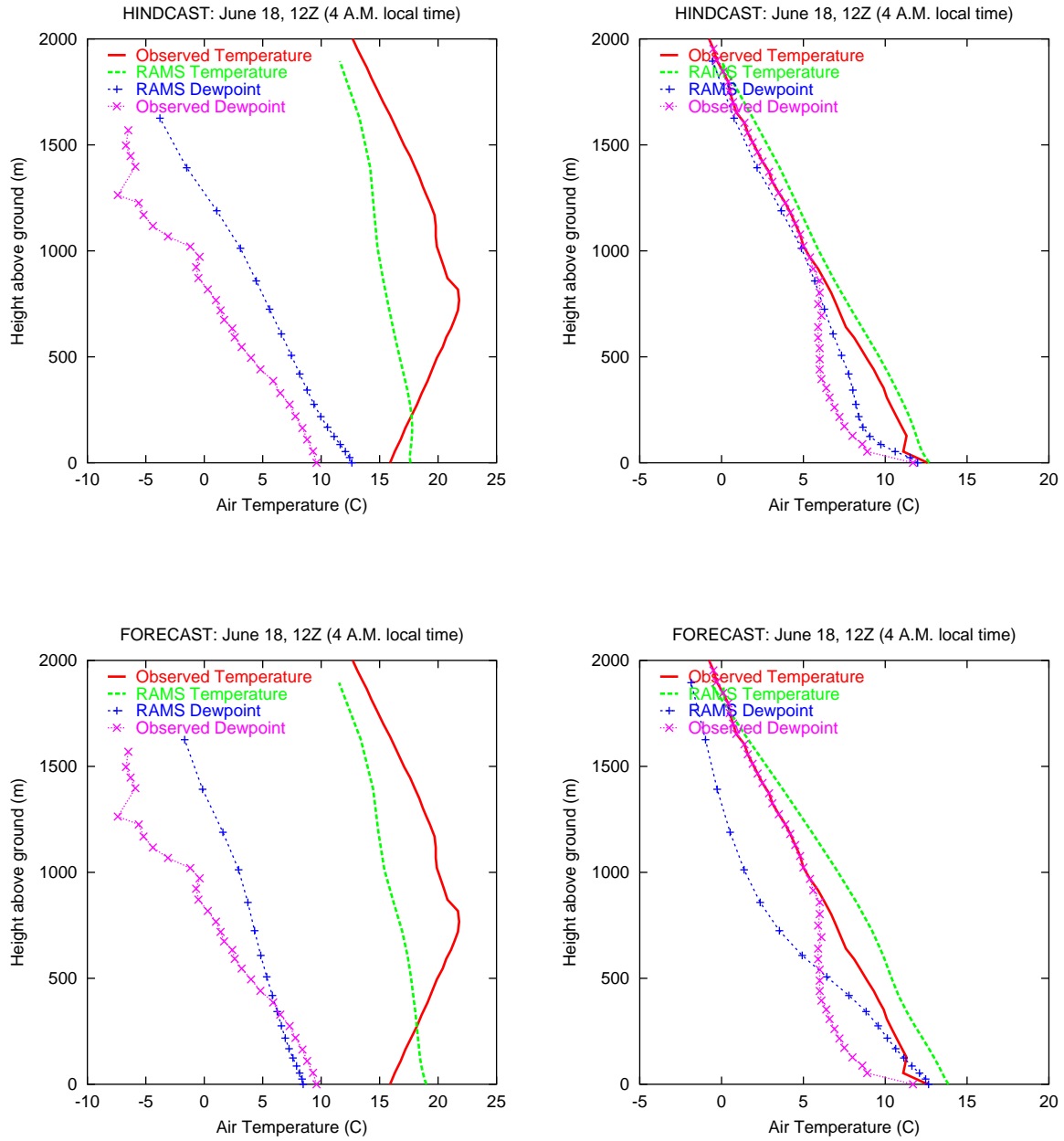


Figure 11: Example Modelled and Observed soundings, Summer Simulation

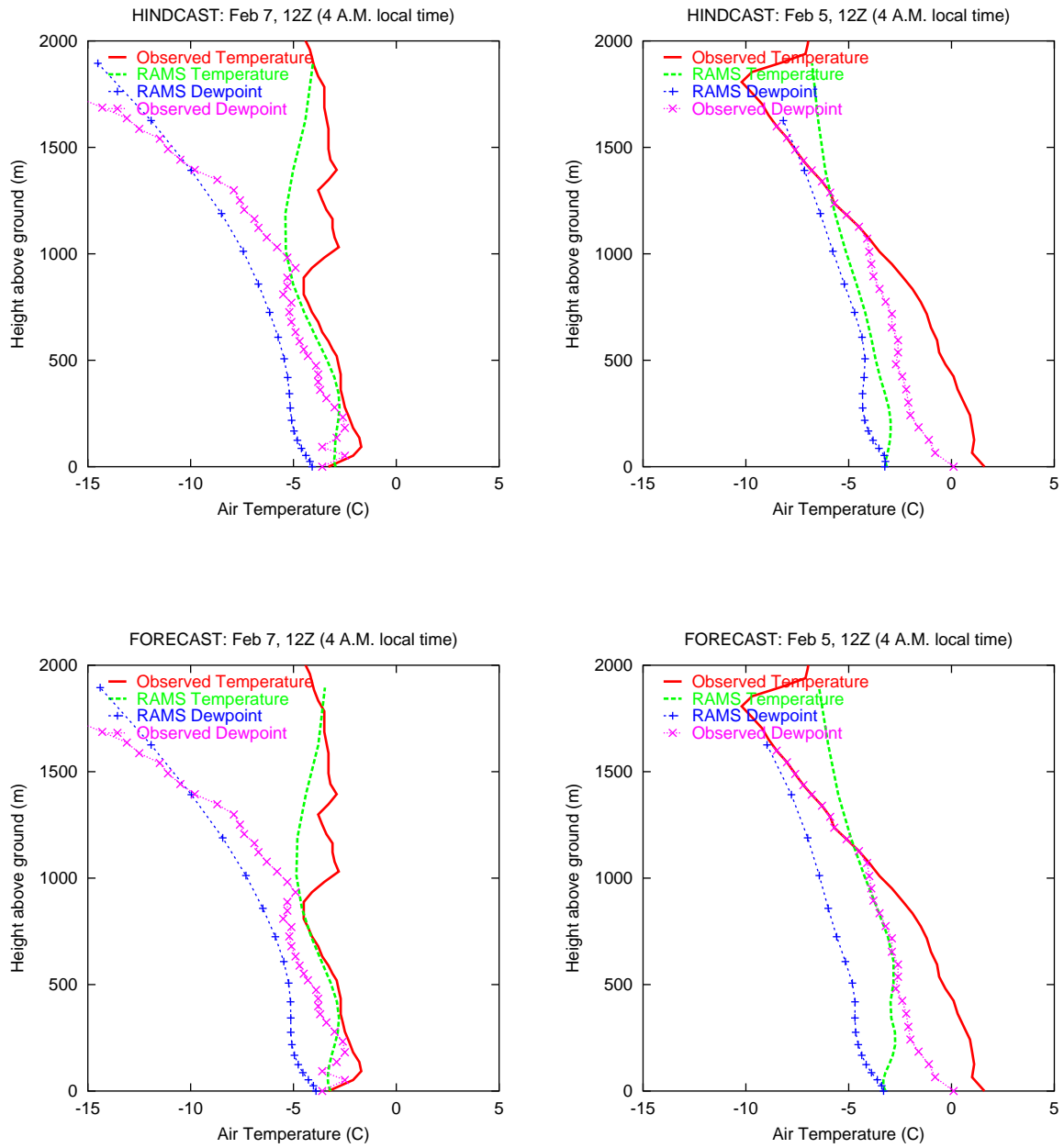


Figure 12: Example Modelled and Observed soundings, Winter Simulation

5 Discussion

The RAMS model was used to simulate meteorological conditions during two periods of episodic air quality conditions in the Thomson-Okanagan area of British Columbia. The model was initialized and nudged with 90 km ETA fields only; no local station observations were used. Two different strategies were used to nudge the RAMS model during simulations; HINDCAST used ETA analysed fields every 6 hours and FORECAST used ETA forecast fields every 3 hours. Both strategies were able to reproduce observed wind patterns at most surface station locations, with HINDCAST fields marginally better than FORECAST. The two periods, one during the summer and the other during winter, were challenging to model. During calm conditions, synoptic-scale influences, which the model fully represents, can have less influence on surface winds than local sub-grid scale features. The analysis showed that there was considerable spatial and temporal variation in both the observed and simulated winds.

Surface and upper-air validation of the simulated fields showed that strengths and weaknesses of the two strategies were very similar. Although wind comparisons generally favoured HINDCAST, in most situations the difference in correlation values for the two modelling strategies was not significant at the 95% confidence interval. Modelled and observed surface station winds were not highly correlated at several locations and times, indicating possible limitations for the use of such fields with real-time forecasting of air quality. However, wind field plots indicated that model timing of shifts in circulation patterns was partly responsible for these low correlations.

The error in modelled surface fields are similar in magnitude to what other studies have found (e.g. Henmi, 2000). RAMS at 1 km resolution produced wind fields with lower error than those at 3 km resolution, but only noticeably with HINDCAST. This study suggests that there is an improvement in statistical simulation skill when reducing model horizontal spacing from 3 km to 1 km, but the improvement is not large. This conclusion may not hold true for a different region, especially one with relatively flat terrain. Such a benefit has to be weighed against increases in computer simulation time; it was observed in this study that dropping grids 5 and 6 from the modelling domain would decrease run times by a factor of 2 or more.

Qualitative assessments added some important insights to the characteristics of the modelled fields. In particular, windrose diagrams showed that both modelling strategies were able to

reproduce station observations at most locations, even at times when correlation values were low. The windrose diagrams also indicated that simulated winds can be a poor representation of observations for some locations and times. Smaller scale terrain features that RAMS cannot represent at 1 km resolution would be responsible for some of this trouble. Whether or not observations at these (or any) locations are an appropriate measure of the wind field of the area could not be addressed in this study. A visual assessment of each surface station location, with accompanying nearby terrain features, would lead to a better understanding of why agreement was better at some locations than others. Future simulation studies in the Thomson-Okanagan area would benefit from this information.

Observed and modelled vertical temperature profiles showed that RAMS had difficulty in reproducing inversion conditions in Kelowna, although agreement was relatively good during neutral and convective conditions. This was not unexpected, as other studies have found this same limitation. The ETA fields used for initialization and nudging do not resolve boundary layer features, so a mesoscale model must develop these features as it progresses through a simulation. RAMS may produce too much vertical mixing during stable conditions, which wouldn't allow a strong inversion to develop. The use of one or more upper air stations with the coarse model (ETA) fields during data assimilation for RAMS could improve this deficiency. It would be very useful to compare boundary layer features of the RAMS simulations with fields developed by another model such as the Mesoscale Community 2 (MC2). Further research needs to be done in this area.

The results of this study show that high resolution fields from a numerical model could be very useful in situations where small differences between observed and simulated timing is not important. For example, the fields would be appropriate for regulatory, or longer term dispersion modelling of an area. However, in an area of complex terrain, some adjustment to better represent inversion conditions may be needed. Using a mix of simulated surface winds with measured temperature profiles likely would be more appropriate than using the full simulations 'as is'. Simulation skill was measured to be higher when using RAMS with analysed ETA fields compared to forecast ETA fields. The difference between simulated fields from the two modelling strategies is small, as they possess similar strengths and weaknesses.

6 References

- Cox, R.M., J. Sontowski, R.N. Fry Jr., C.M. Dougherty and T.J. Smith, 1998a: Wind and Diffusion Modeling for Complex Terrain. *J. Appl. Met.*, **37**, 996-1009.
- Cox, R., B.L. Bauer, and T. Smith, 1998b: A Mesoscale Model Intercomparison. *Bulletin of the American Meteorological Society*, **79**, 265-283.
- Henmi, T, 2000: The Comparison and Evaluation of Operational Mesoscale Models MM5 and BFM over White Sands Missile Range. US Army Research Laboratory Technical Report ARL-TR-1476.
- Holton, J.R., 1979: *An Introduction to Dynamic Meteorology*, Second Edition. Academic Press Limited, San Diego, California, 391 pp.
- Lyons, W.A., C.J. Tremback and R.A. Pielke, 1995: Applications of the Regional Atmospheric Modeling System (RAMS) to Provide Input to the Photochemical Grid Models for the Lake Michigan Ozone Study (LMOS). *J. Appl. Met.*, **34**, 1762-1786.
- McQueen, J.T., R.R. Draxler, and G.D. Rolph, 1995: Influence of Grid Size and Terrain Resolution on Wind Field Predictions from an Operational Mesoscale Model. *J. Appl. Met.*, **34**, 2166-2180.
- Pielke, R. A., W. R. Walko, C. J. Tremback, W. A. Lyons, L. D. Grasso, M. E. Nicholls, M. D. Moran, D. A. Wesley, T. J. Lee and J. H. Copeland, 1992: A Comprehensive Meteorological Modeling System - RAMS. *Meteor. Atmos. Phys.*, **49**, 69-91.
- Pielke, R. A. and M. Uliasz, 1998: Use of Meteorological Models As Input To Regional and Mesoscale Air Quality Models - Limitations and Strengths. *Atmospheric Environment*, **32**, 1455-1466.
- Stull, R.B., 1995: *Meteorology Today For Scientists and Engineers*. West Publishing Company, St. Paul, MN, 385 pp.
- Walko R.L. and C.J. Tremback, 1999: *Regional Atmospheric Modelling System Version 4.2, Introduction to RAMS 4.2*. <http://www.atmet.com>.
- Willmott, C.J., S.G. Ackleson, R.E. Davis, J.J. Feddema, K.M. Klink, D.R. Legates, J. O'Donnell, and C.M. Rowe, 1985: Statistics for the Evaluation and Comparison of Models. *Journal of Geophysical Research*, **90**, 8995-9005.

7 Appendix A: RAMS Initialization File

```

!namelist
!##### Change Log #####
! RAMS Initialization file for FORECAST run June 12, 2002
!
!#####

$MODEL_GRIDS

! Simulation title (64 chars)

EXPNAME = 'June 12 - 26 run using analysed Eta fields',
VTABCUST = 'standard',

RUNTYPE = 'MAKESFC', ! Type of run: MEMORY, MAKESFC, MAKESST,
! MAKEVFILE, INITIAL, HISTORY

TIMEUNIT = 'h', ! 'h','m','s' - Time units of TIMMAX, TIMSTR

TIMMAX = 21., ! Final time of simulation

! Start of simulation or ISAN processing

IMONTH1 = 06, ! Month
IDATE1 = 12, ! Day
IYEAR1 = 2002, ! Year
ITIME1 = 0000, ! GMT of model TIME = 0.

! Grid specifications

NGRIDS = 6,

NNXP = 60,62,62,74,62,62, ! Number of x gridpoints
NNYP = 60,62,62,83,98,62, ! Number of y gridpoints
NNZP = 40,40,40,40,40,40, ! Number of z gridpoints
NZG = 11,11,11,11,11,11, ! Number of soil layers
NZZ = 1,1,1,1,1,1, ! Maximum number of snow layers

NXTNEST = 0,1,2,3,4,4, ! Grid number which is the next
coarser grid

! Coarse grid specifications

IHTRAN = 1, ! 0-Cartesian, 1-Polar stereo
DELTAX = 81000.,
DELTAY = 81000., ! X and Y grid spacing

DELTAZ = 25., ! Z grid spacing (set to 0. to use ZZ)
DZRAT = 1.15, ! Vertical grid stretch ratio
DZMAX = 1000., ! Maximum delta Z for vertical stretch

ZZ = 0.0, ! Vertical levels if DELTAZ = 0
30.0, 60.0, 90.0, 120.0, 150.0,
180.0, 210.0, 240.0, 270.0, 300.0,
330.0, 360.0, 390.0, 420.0, 450.0,
480.0, 510.0, 540.0, 570.0, 600.0,
630.0, 660.0, 690.0, 720.0, 750.0,
780.0, 810.0, 840.0, 870.0, 900.0,
930.0, 960.0, 990.0, 1020.0, 1050.0,
1080.0, 1110.0, 1140.0, 1170.0, 1200.0,
1230.0, 1260.0, 1290.0, 1320.0, 1350.0,
1380.0, 1410.0, 1440.0, 1470.0, 1500.0,
1533.0, 1569.3, 1609.2, 1653.2, 1701.5,
1754.6, 1813.1, 1877.4, 1948.1, 2025.9,
2111.5, 2205.7, 2309.3,

DTLONG = 120., ! Coarse grid long timestep (if IDELTAT=0)
NACOUST = 4, ! Small timestep ratio (inv. porportional)
IDELTAT = -2, ! Timestep adjustment
! =0 - constant timesteps (otherwise auto)
! >0 - initial computation <0 - variable

! Nest ratios between this grid and the next
! coarser grid.
NSTRATX = 1,3,3,3,3,3, ! x-direction
NSTRATY = 1,3,3,3,3,3, ! y-direction
NNDTRAT = 1,3,3,3,3,3, ! Time

NESTZ1 = 0, ! Contort coarser grids if -ve, if 0 no nest
NSTRATZ1 = 1,3,3,3,2,2,1,
NESTZ2 = 0, ! Contort coarser grids if -ve, for global
NSTRATZ2 = 3,3,3,2,2,1,

POLELAT = 50.0, ! Latitude of pole point
POLELON = -119.6, ! Longitude of pole point

CENTLAT = 50.0,50.0,50.0,50.283,49.865,50.725, ! Center lat/lon of
grids, may or
CENTLON = -119.6,-119.6,-119.6,-119.854,-119.474,-120.538, ! may
not be
same as pole point.

```

```

! Grid point on the next coarser
! nest where the lower southwest
! corner of this nest will start.
! If NINEST or NJNEST = 0, use CENTLAT/LON
NINEST = 1,20,21,17,36,11,      ! i-point
NJNEST = 1,20,21,21,10,48,     ! j-point
NKNEST = 1,1,1,1,1,1,         ! k-point

NNSTTOP = 1,1,1,1,1,1,        ! Flag (0=no or 1=yes) if this
NNSTBOT = 1,1,1,1,1,1,        ! Nest goes the top or bottom of the
! coarsest nest.

GRIDU = 0.,0.,                ! u-component for moving grids
GRIDV = 0.,0.,                ! v-component for moving grids
! (still not working!)

$END

$MODEL_FILE_INFO

! Variable initialization input

INITIAL = 2,                   ! Initial fields - 1=horiz.homogeneous,
!                               2=variable
VARFPFX = 'isan/a',           ! Varfile initialization file prefix
VWAIT1 = 0.,                  ! Wait between each VFILE check (s)
VWAITTOT = 0.,                ! Total wait before giving up on a VFILE (s)

NUDLAT = 5,                   ! Number of points in lateral bnd region
TNUDLAT = 1800.,
TNUDCENT = 12000.,
domain
TNUDTOP = 00.,                ! Nudging time scale (s) at top of domain
ZNUDTOP = 15000.,            ! Nudging at top of domain above height(m)

! History file input

TIMSTR = 12.,                 ! Time of history start (see TIMEUNIT)
HFILIN = 'hist/a-H-2002-06-12-000000.vfm',
! Input history file name

! History/analysis file output

IOUOUTPUT = 2,                ! 0=no files, 1=save ASCII, 2=save binary
HFILOUT = 'hist/a',           ! History file prefix
AFILOUT = 'anal/a',           ! Analysis file prefix
ICLOBBER = 1,                 ! 0=stop if files exist, 1=overwrite files
IHISTDEL = 1,                 ! 0=keep all hist files, 1=delete previous
FRQHIS = 43200.,              ! History file frequency (every 6 hrs)
FRQANL = 21600.,              ! Analysis file frequency
FRQLITE = 3600.,              ! Analysis freq. for "lite" variables
! = 0 : no lite files
XLITE = '/0:0/',              ! nums>0 are absolute grid indexes
YLITE = '/0:0/',              ! nums<0 count in from the domain edges
ZLITE = '/0:0/',              ! nums=0 are domain edges
AVGTIM = 0.,                  ! Averaging time for analysis variables
! must be abs(AVGTIM) <= FRQANL
! > 0 : averaging is centered at FRQANL
! < 0 : averaging ends at FRQANL
! = 0 : no averaged files
FRQMEAN = 0.,                 ! Analysis freq. for "averaged" variables
FRQBOTH = 0.,                 ! Analysis freq. for both "averaged" and
! "lite" variables
KWRITE = 0,                   ! 1=write,0=don't write scalar K's to anal.

! Printed output controls

FRQPRT = 10800.,              ! Printout frequency
INITFLD = 0,                  ! Initial field print flag 0=no prnt,1=prnt

! Input topography variables

SFCFILES = 'sfc/sfc',         ! File path and prefix for surface files.
SSTFPFX = 'sst/sst',          ! Path and prefix for sst files

ITOPTFLG = 1,1,1,1,1,1,      ! 2 - Fill data in "rsurf"
ISSTFLG = 1,1,1,2,2,2,        ! 0 - Interpolate from coarser grid
IVEGTFGL = 1,1,1,1,1,1,      ! 1 - Read from standard Lat/Lon data
file
ISOILFLG = 2,2,2,2,2,2,      ! Soil files not yet available: avoid
isoilflg=1

NOFILFLG = 2,2,2,2,2,2,      ! 2 - Fill data in "rsurf"
! 0 - Interpolate from coarser grid

IUPDSSST = 0,                 ! 0 - No update of SST values during run
! 1 - Update SST values during run

! The following only apply for IxxxxFLG=1
ITOPTFN = '/scratch2/atmos/rams/geodata/topo10m/H',

```

```

        '/scratch2/atmos/rams/geodata/DEM30snew/EL',
        '/scratch2/atmos/rams/geodata/DEM30snew/EL',
        '/scratch2/atmos/rams/geodata/DEM30snew/EL',
        '/scratch2/atmos/rams/geodata/DEM30snew/EL',
        '/scratch2/atmos/rams/geodata/DEM30snew/EL',
ISSTFN = '/scratch2/atmos/rams/geodata/sst43/S',
        '/scratch2/atmos/rams/geodata/sst43/S',
        '/scratch2/atmos/rams/geodata/sst43/S',
        '/scratch2/atmos/rams/geodata/sst43/S',
        '/scratch2/atmos/rams/geodata/sst43/S',
        '/scratch2/atmos/rams/geodata/sst43/S',
IVEGTFN = '/scratch2/atmos/rams/geodata/ogedata/GE',
        '/scratch/mcewenb/data/ogedata/GE',
        '/scratch/mcewenb/data/ogedata/GE',
        '/scratch/mcewenb/data/ogedata/GE',
        '/scratch/mcewenb/data/ogedata/GE',
        '/scratch/mcewenb/data/ogedata/GE',
        '/scratch/mcewenb/data/ogedata/GE',
ISOILFN = ' ',          ! Soil files not yet available

! Topography scheme
ITOPSFGL = 3,3,3,3,3,3,          ! 0 = Average Orography
        ! 1 = Silhouette Orography
        ! 2 = Envelope Orography
        ! 3 = Reflected Envelope Orography
TOPTENH = 1.,1.,1.,1.,1.,1.,1.,          ! For ITOPSFGL=1, Weighting of topo
        ! silhouette averaging
        ! For ITOPSFGL=2 or 3, Reflected Envelope
        ! and Envelope Orography enhancement factor
TOPTWVL = 4.,4.,4.,4.,4.,4.,          ! Topo wavelength cutoff in filter

! Surface Roughness scheme
IZOFLG = 0,0,0,0,0,0,          ! 0 = Based of vege, bare soil and
water surface                   ! 1 = Subgrid scale orographic roughness
ZOMAX = 2.,2.,2.,2.,2.,2.,          ! Max zo for IZOFLG=1
ZOFACT = 0.005,          ! Subgrid scale orographic roughness factor

! Microphysics collection tables
MKCOLTAB = 0,          ! Make table: 0 = no, 1 = yes
COLTABFN = '/scratch2/atmos/rams/geodata/micro43/ct2.0',
        ! Filename to read or write

$END

$MODEL_OPTIONS
NADDSC = 0,          ! Number of additional scalar species

! Numerical schemes
ICORFLG = 1,          ! Coriolis flag/2D v-component - 0 = off, 1 = on

IBND = 2,          ! Lateral boundary condition flags
JBND = 2,          ! 1-Klemp/Wilhelmson, 2-Klemp/Lilly,
        ! 3-Orlanski, 4-cyclic
CPHAS = 20.,          ! Phase speed if IBND or JBND = 1
LSPLG = 0,          ! Large-scale gradient flag for variables other than
        ! normal velocity:
        ! 0 = zero gradient inflow and outflow
        ! 1 = zero gradient inflow, radiative b.c. outflow
        ! 2 = constant inflow, radiative b.c. outflow
        ! 3 = constant inflow and outflow
NFPT = 0,          ! Rayleigh friction - number of points from the top
DISTIM = 60.,          ! - dissipation time scale

! Radiation parameters
ISWRTYP = 1,
ILWRTYP = 1,          ! 0-none, 2-Mahrer/Pielke, 1-Chen
RADFRQ = 1200.,
LONRAD = 1,          ! Longitudinal variation of shortwave
        ! (0-no, 1-yes)

! Cumulus parameterization parameters
NNQPARM = 1,
CONFRQ = 1200.,          ! Frequency of conv param. updates (s)
WCLDBS = .001,          ! Vertical motion needed at cloud base for
        ! to trigger convection

! Surface layer and soil parameterization
NPATCH = 3,          ! Number of patches per grid cell (min=2)

```

```

NVEGPAT = 2,          ! Number of patches per grid cell to be filled from
                   ! vegetation files (min of 1, max of NPATCH-1)

ISFCL   = 1,          ! 0 - specified surface layer gradients
                   ! 1 - soil/vegetation model

NVGCON  = 10,        ! Vegetation type (see below)

! 0 Ocean              1 Lakes rivers streams (inland water)
! 2 Ice cap/glacier    3 Evergreen needleleaf tree
! 4 Deciduous needleleaf tree 5 Deciduous broadleaf tree
! 6 Evergreen broadleaf tree 7 Short grass
! 8 Tall grass         9 Desert
! 10 Semi-desert      11 Tundra
! 12 Evergreen shrub  13 Deciduous shrub
! 14 Mixed woodland  15 Crop/mixed farming
! 16 Irrigated crop  17 Bog or marsh
! 18 Evergreen needleleaf forest 19 Evergreen broadleaf forest
! 20 Deciduous needleleaf forest 21 Deciduous broadleaf forest
! 22 Mixed cover      23 Woodland
! 24 Wooded grassland 25 Closed shrubland
! 26 Open shrubland  27 Grassland
! 28 Cropland        29 Bare ground
! 30 Urban and built up

PCTLCON = 1.,        ! Constant land % if for all domain
NSLCON  = 6,         ! Constant soil type if for all domain

! 1 sand              2 loamy sand   3 sandy loam
! 4 silt loam        5 loam         6 sandy clay loam
! 7 silty clay loam  8 clay loam   9 sandy clay
! 10 silty clay      11 clay        12 peat

ZROUGH  = 0.1,        ! Constant roughness if for all domain
ALBEDO  = .2,         ! Constant albedo if not running soil model
SEATMP  = 288.,       ! Constant water surface temperature

DTHCON  = 0.,        ! Constant sfc layer temp grad for no soil
DRTCEN  = 0.,        ! Constant sfc layer moist grad for no soil

SLZ     = -.50,-.40,-.30,-.25,-.20,-.16,-.12,-.09,-.06,-.03,-.01,
                   ! Soil grid levels

SLMSTR  = 0.5,0.45,0.4,0.35,0.35,0.35,0.3,0.3,0.3,0.25,0.2,
                   ! Initial soil moisture

STGOF   = 5.,5.,5.,5.,3.5,2.,.5,-1.,-1.5,-1.8,-2.,
                   ! Initial soil temperature offset
                   ! from lowest atmospheric level
! Eddy diffusion coefficient parameters

IDIFFK  = 1,1,1,1,1,1,          ! K flag:
                   ! 1 - Horiz deform/Vert Mellor-Yamada
                   ! 2 - Anisotropic deformation
                   ! (horiz & vert differ)
                   ! 3 - Isotropic deformation
                   ! (horiz and vert same)
                   ! 4 - Deardorff TKE (horiz and vert same)
IHORGRAD = 2,                  ! 1 - horiz grad frm decomposed sigma grad
                   ! 2 - true horizontal gradient.
                   ! Non-conserving, but allows small DZ
CSX     = .32,.32,.32,.32,.32,.32,          ! Deformation horiz. K's
coefficient
CSZ     = .2,.2,.2,.2,.2,.2,                ! Deformation vert. K's
coefficient
XKHKM  = 3.,3.,3.,3.,3.,3.,                ! Ratio of horiz K_h to K_m for
deformation
ZKHKM  = 3.,3.,3.,3.,3.,3.,                ! Ratio of vert K_h to K_m for
deformation
AKMIN  = 1.0,1.0,1.0,1.0,1.0,1.0,          ! Ratio of minimum horizontal
eddy
                   ! viscosity coefficient to typical value
                   ! from deformation K

! Microphysics

LEVEL  = 3,          ! Moisture complexity level
ICCNFLG = 0,         ! Flag for CCN and IF
IFNFLG = 0,         ! 0-constant,1-vertical profile,2-prognosed

ICLOUD = 4,         ! Microphysics flags
IRAIN  = 2,         !-----
IPRIS  = 5,         ! 1 - diagnostic concn.
ISNOW  = 2,         ! 2 - specified mean diameter
IAGGR  = 2,         ! 3 - specified y-intercept
IGRAUP = 2,         ! 4 - specified concentration
IHAILE = 2,         ! 5 - prognostic concentration

CPARM  = .3e9,       ! Microphysics parameters
RPARM  = 1e-3,       !-----

```

```

PPARM = 0.,          ! Characteristic diameter, # concentration
SPARM = 1e-3,       ! or y-intercept
APARM = 1e-3,
GPARM = 1e-3,
HPARM = 3e-3,

GNU = 2.,2.,2.,2.,2.,2.,2.,2., ! Gamma shape parms for
! cld rain pris snow aggr graup hail

$END

$MODEL_SOUND
!-----
! Sounding specification
!-----
! Flags for how sounding is specified

IPSFGL = 1,          ! Specifies what is in PS array
! 0-pressure(mb) 1-heights(m)
! PS(1)=sfc press(mb)

ITSFGL = 0,          ! Specifies what is in TS array
! 0-temp(C) 1-temp(K) 2-pot. temp(K)

IRTSFGL = 3,         ! Specifies what is in RTS array
! 0-dew pnt.(C) 1-dew pnt.(K)
! 2-mix rat(g/kg)
! 3-relative humidity in %,
! 4-dew pnt depression(K)

IUSFGL = 0,          ! Specifies what is in US and VS arrays
! 0-u,v component(m/s)
! 1-umoms-direction, vmoms-speed

HS = 0.,

PS = 1010.,1000.,2000.,3000.,4000.,6000.,8000.,11000.,15000.,20000.,
25000.,

TS = 25.,18.5,12.,4.5,-11.,-24.,-37.,-56.5,-56.5,-56.5,-56.5,

RTS = 70.,70.,70.,70.,20.,20.,20.,20.,10.,10.,10.,

US = 10.,10.,10.,10.,10.,10.,10.,10.,10.,10.,10.,

VS = 0.,0.,0.,0.,0.,0.,0.,0.,0.,0.,0.,

$END

$MODEL_PRINT
!-----
! Specifies the fields to be printed during the simulation
!-----

NPLT = 4,            ! Number of fields printed at each time
! for various cross-sections (limit of 50)

IPLFLD = 'UP','VP','WP','THETA','RELHUM','TOTPRE',
! Field names - see table below

! PLFMT(1) = '0PF7.3', ! Format spec. if default is unacceptable

IXSCTN = 3,3,3,3,3,3, ! Cross-section type (1=XZ, 2=YZ, 3=XY)

ISBVAL = 10,10,10,10,10,10,
! Grid-point slab value for third direction

! The following variables can also be set in the namelist: IAA,
! IAB, JOA, JOB, NAAVG, NOAVG, PLTIT, PLCONLO, PLCONHI, and PLCONIN.

! 'UP' - UP(M/S) 'RC' - RC(G/KG) 'PCPT' - TOTPRE
! 'VP' - VP(M/S) 'RR' - RR(G/KG) 'TKE' - TKE
! 'WP' - WP(CM/S) 'RP' - RP(G/KG) 'HSCL' - HL(M)
! 'PP' - PRS(MB) 'RA' - RA(G/KG) 'VSCL' - VL(M)
! 'THP' - THP(K)
! 'THETA' - THETA(K) 'RL' - RL(G/KG) 'TG' - TG (K)
! 'THVP' - THV(K) 'RI' - RI(G/KG) 'SLM' - SLM (PCT)
! 'TV' - TV(K) 'RCOND' - RD(G/KG) 'CONPR' - CON RATE
! 'RT' - RT(G/KG) 'CP' - NPRIS 'CONP' - CON PCP
! 'RV' - RV(G/KG) 'RTP' - RT(G/KG) 'CONH' - CON HEAT
! 'CONM' - CON MOIS
! 'THIL' - Theta-il (K) 'TEMP' - temperature (K)
! 'TVP' - Tv (K) 'THV' - Theta-v (K)
! 'RELHUM' - relative humidity (%) 'SPEED' - wind speed (m/s)
! 'FTHRD' - radiative flux convergence (??)
! 'MICRO' - GASPRC

```

```

! 'Z0' - Z0 (M) 'ZI' - ZI (M) 'ZMAT' - ZMAT (M)
! 'USTARL'-USTARL(M/S) 'USTARW'-USTARW(M/S) 'TSTARL'-TSTARL (K)
! 'TSTARW'-TSTARW(K) 'RSTARL'-RSTARL(G/G) 'RSTARW'-RSTARW(G/G)
! 'UW' - UW (M*M/S*S) 'VN' - VW (M*M/S*S)
! 'WFZ' - WFZ (M*M/S*S) 'TFZ' - TFZ (K*M/S)
! 'QFZ' - QFZ (G*M/G*S) 'RLONG'- RLONG
! 'RSHORT'-RSHORT

$END

$ISAN_CONTROL

!-----
! Isentropic control
!-----

ISZSTAGE = 1, ! Main switches for isentropic-sigz
IVRSTAGE = 1, ! "varfile" processing

ISAN_INC = 0300, ! ISAN processing increment (hmmm)
! range controlled by TIMMAX,
! IYEAR1,...,ITIME1

GUESS1ST = 'PRESS', ! Type of first guess input- 'PRESS', 'RAMS'

I1ST_FLG = 2, ! What to do if first guess file should be used,
! but does not exist.
! 1 = I know it may not be there,
! skip this data time
! 2 = I screwed up, stop the run
! 3 = interpolate first guess file from nears ! surrounding times, stop if unable
! (not yet available)

IUPA_FLG = 3, ! UPA-upper air, SFC-surface
ISFC_FLG = 3, ! What to do if other data files should be used,
! but does not exist.
! 1 = I know it may not be there,
! skip this data time
! 2 = I screwed up, stop the run
! 3 = Try to continue processing anyway

! Input data file prefixes

IAPR = '/scratch2/atmos/utills/bryan/forecastjunfiles/dp-p',
IARAWI = 'NO/scratch2/atmos/data/ubc_data_20020119/initial_rams/dp-r', ! Archived rawindsonde
IASRFCE = 'NO/scratch2/atmos/data/ubc_data_20020119/initial_rams/dp-s', ! Archived surface obs

! File names and dispose flags

VARPFX = './isan/a', ! isan file names prefix
IOPLGISZ = 0, ! Isen-sigz file flag: 0 = no write, 1 = write
IOPLGVAR = 1, ! Var file flag: 0 = no write, 1 = write

$END

$ISAN_ISENTROPIC

!-----
! Isentropic and sigma-z processing
!-----

!-----
! Specify isentropic levels
!-----

NISN = 63, ! Number of isentropic levels
LEVTH = 270,271,272,273,274,275,276,277,278,279,280,281,282,283,284,
285,286,287,288,289,290,291,292,293,
294,295,296,297,298,299,300,302,304,306,309,312,
315,318,321,324,327,330,335,340,345,350,355,360,380,400,420,
440,460,480,500,520,540,570,600,630,670,700,750,

!-----
! Analyzed grid information:
!-----

NIGRIDS = 6,

TOPSIGZ = 2000., ! Sigma-z coordinates to about this height

HYBBOT = 4000., ! Bottom (m) of blended sigma-z/isentropic
! layer in varfiles
HYBTOP = 6000., ! Top (m) of blended sigma-z/isentropic layr

SFCINF = 1000., ! Vert influence of sfc observation analysis

SIGZWT = 1., ! Weight for sigma-z data in varfile:
! 0. = no sigz data,
! 1. = full weight from surface to HYBBOT

NFEEDVAR = 1, ! 1 = feed back nested grid varfile, 0 = not

```

```

!-----
! Observation number limits:
!-----

MAXSTA = 500,          ! maximum number of rawinsondes
                    ! (archived + special)
MAXSFC = 5000,        ! maximum number of surface observations

NONLYS = 0,           ! Number of stations only to be used
IDONLYS = '76458',    ! Station IDs used

NOTSTA = 0,           ! Number of stations to be excluded
NOTID = 'r76458',     ! Station IDs to be excluded
                    ! Prefix with 'r' for rawinsonde,
                    ! 's' for surface

IOBSWIN = 7200,       ! Observation acceptance time window
                    ! Obs are accepted at the analysis time T if
                    ! for IOBSWIN > 0: T-IOBSWIN < obs_time < T+IOBSWIN
                    ! for IOBSWIN = 0: T = obs_time
                    ! for IOBSWIN < 0: T-|IOBSWIN| < obs_time

STASEP = .1,          ! Minimum sfc station separation in degrees.
                    ! Any surface obs within this distance
                    ! of another obs will be thrown out
                    ! unless it has less missing data,
                    ! in which case the other obs will be
                    ! thrown out.

ISTAPLT = 0,          ! If ISTAPLT = 1, soundings are plotted;
ISTAREP = 0,          ! If ISTAREP = 1, soundings are listed;
                    ! no objective analysis is done.
                    ! If ISTAREP/ISTAPLT = 0, normal processing
                    ! is done

IGRIDFL = 3,          ! Grid flag=0 if no grid point, only obs
                    ! 1 if all grid point data and obs
                    ! 2 if partial grid point and obs
                    ! 3 if only grid data
                    ! 4 all data... fast

GRIDWT = .01,.01,.01,.01, ! Relative weight for the gridded press data
                    ! compared to the observational data in
                    ! the objective analysis

GOBSEP = 5.,          ! Grid-observation separation (degrees)
GOBRAD = 5.,          ! Grid-obs proximity radius (degrees)

WVLNTH = 1200.,900.,900.,900.,900., ! Used in S. Barnes objective analysis.
                    ! Wavelength in km to be retained to the
                    ! RESPON % from the data to the upper air
                    ! grids.
SWVLNTH = 750.,300.,300.,300.,300., ! Wavelength for surface objective analysis

RESPON = .90,.9,.9,.9,.9, ! Percentage of amplitude to be retained.

$END

!-----
! Graphical processing
!-----

$ISAN_GRAPH

! Main switches for plotting

IPLTPRS = 0,          ! Pressure coordinate horizontal plots
IPLTISN = 0,          ! Isentropic coordinate horizontal plots
IPLTSIG = 0,          ! Sigma-z coordinate horizontal plots
IPLTSTA = 0,          ! Isentropic coordinate "station" plots

!-----
! Pressure plotting information
!-----

ILFTL1 = 0,           ! Left boundary window
IRGTL1 = 18,          ! Right boundary window
IBOTL1 = 3,           ! Bottom boundary window
ITOPL1 = 13,          ! Top boundary window
                    ! Window defaults to entire domain if one equals 0.

NPLEV = 2,            ! Number of pressure levels to plot
IPLEV = 1000,500,     ! Levels to be plotted
                    ! Levels to be plotted
NFLDU1 = 4,           ! Number of fields to be plotted
IFLDU1 = 'U','THETA','GEO','RELHUM', ! Field names
CONU1 = 0.,0.,0.,0., ! Field contour increment
IVELU1 = 2,0,0,0,     ! Velocity vector flag

!-----

```

```

! Isentropic plotting information
!-----
      ILFT3I = 0,          ! Left boundary window
      IRGT3I = 18,         ! Right boundary window
      IBOT3J = 3,          ! Bottom boundary window
      ITOP3J = 13,         ! Top boundary window
                          ! Window defaults to entire domain if one equals 0.

! Upper air plots:
      IUP3BEG = 320,       ! Starting isentropic level for plotting
      IUP3END = 380,       ! Ending isentropic level
      IUP3INC = 60,        ! Level increment

      NFLDU3 = 5,          ! Number of fields to be plotted
      IFLDU3 = 'U','V','PRESS','GEO','RELHUM', ! Field names
      CONU3  = 0.,0.,      ! Field contour increment
      IVELU3 = 1,0,        ! Velocity vector flag

!-----
! Surface plotting information
!-----

! Uses isentropic plotting window info
      NFLDS3 = 5,          ! Number of surface fields to plot
      IFLDS3 = 'U','V','PRESS','GEO','RELHUM', ! Field names
      CONS3  = 0.,0.,0.,0., ! Field contour increment
      IVELS3 = 1,0,0,0,    ! Velocity vector flag

!-----
! Sigma-z plotting information
!-----

! Uses isentropic plotting window info
      ISZBEG = 2,          ! Starting sigma-z level for plotting
      ISZEND = 8,          ! Ending sigma-z level
      ISZINC = 6,          ! Level increment

      NFLDSZ = 5,          ! Number of fields to be plotted
      IFLDSZ = 'U','V','PRESS','THETA','RELHUM', ! Field names
      CONSZ  = 0.,0.,      ! Field contour increment
      IVELSZ = 1,0,        ! Velocity vector flag

!-----
! "Station" plotting information
!-----

      NPLTRAW = 25,        ! Approximate number of raw rawinsonde plots
                          ! per frame. 0 turns off plotting.

      NSTIS3 = 2,          ! Number of station surface plots
      ISTIS3 = 'PRESS','RELHUM','MIXRAT', ! Field names

!-----
! Cross-section plotting information
!-----

      NCROSS3 = 0,         ! Number of cross section slabs
      ICRTYP3 = 2,1,       ! Type of slab: 1=E-W, 2=N-S
      ICRA3   = 1,1,       ! Left window
      ICRB3   = 35,43,     ! Right window
      ICRL3   = 22,25,    ! Cross section location
      NCRFLD3 = 3,         ! Number of plots on each cross section
      ICRFLD3 = 'MIXRAT','RELHUM','THETA', ! field names
      THCON3  = 5.,5.,5., ! Contour interval of isentropes
      ACON3   = 0.,0.,0., ! Contour interval of other field

$END

!-----
! Field values for graphical stage
!-----
!
! Pressure      Isentropic    Station      Sigma-z
!-----
! U             U             U             U
! V             V             V             V
! TEMP          PRESS        PRESS        PRESS
! GEO           GEO          TEMP         THETA
! RELHUM        RELHUM       RELHUM       RELHUM
! MIXRAT        MIXRAT       MIXRAT
! THETA         THETA
! SPEED         SPEED
! ENERGY       ENERGY
! THETA         THETA
! SPRESS        SPRESS
!

```

8 Appendix B: Windrose Diagrams

Note: Although the same wind speed categories are used for each plot, the frequency rings are relative to the most frequent wind direction. Frequency percentiles, indicated on each ring, are not the same for every plot.

The first 4 sets of windrose diagrams represent modelled and observed winds at stations with relatively good agreement as determined from statistical comparisons (tables 6 and 7). The last 4 sets of windrose diagrams represent modelled and observed winds at stations with relatively poor statistical agreement.

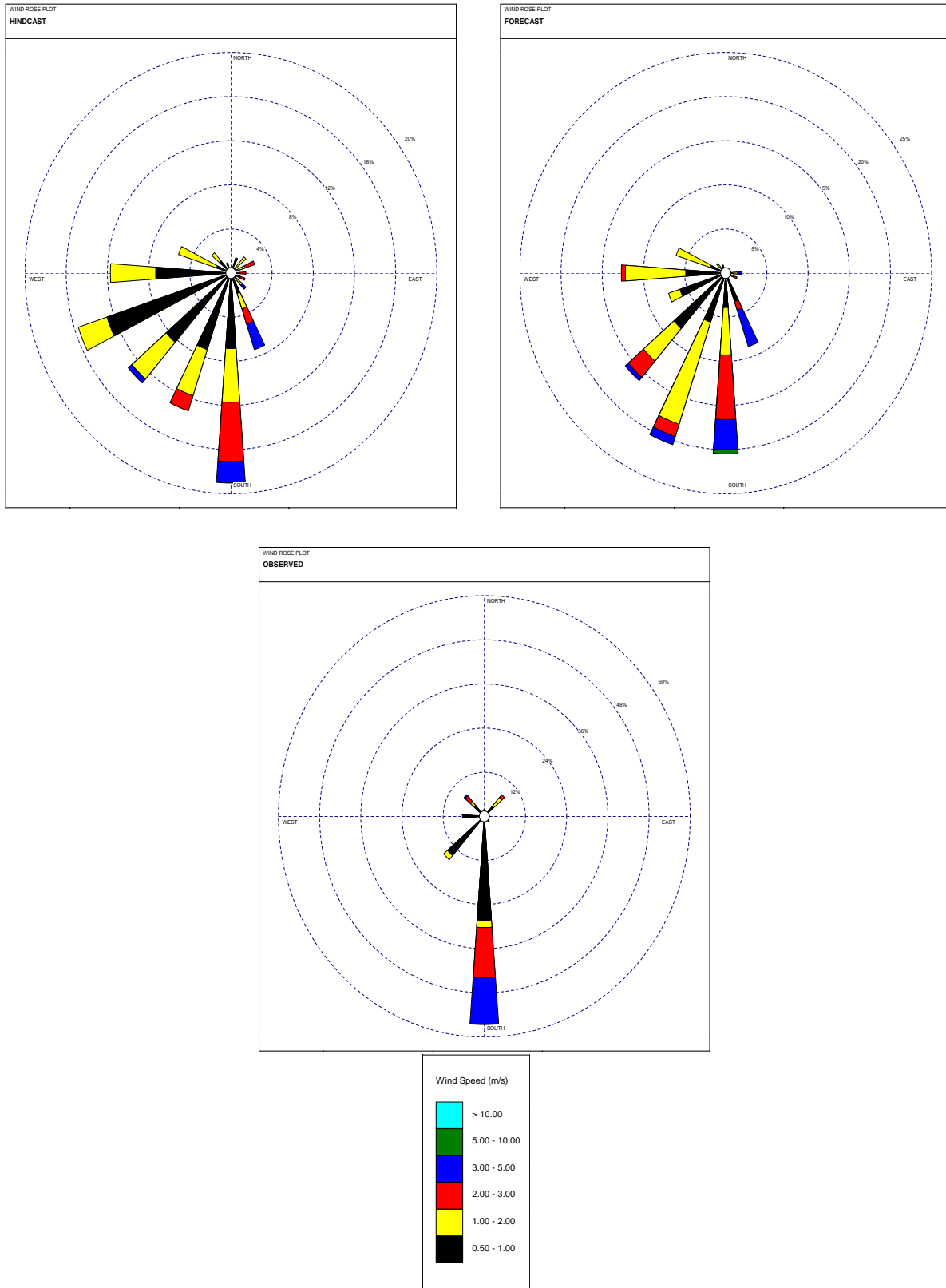


Figure 13: Windrose diagrams showing observed and modelled surface winds for the duration of the summer simulation at MoF-2035 station.

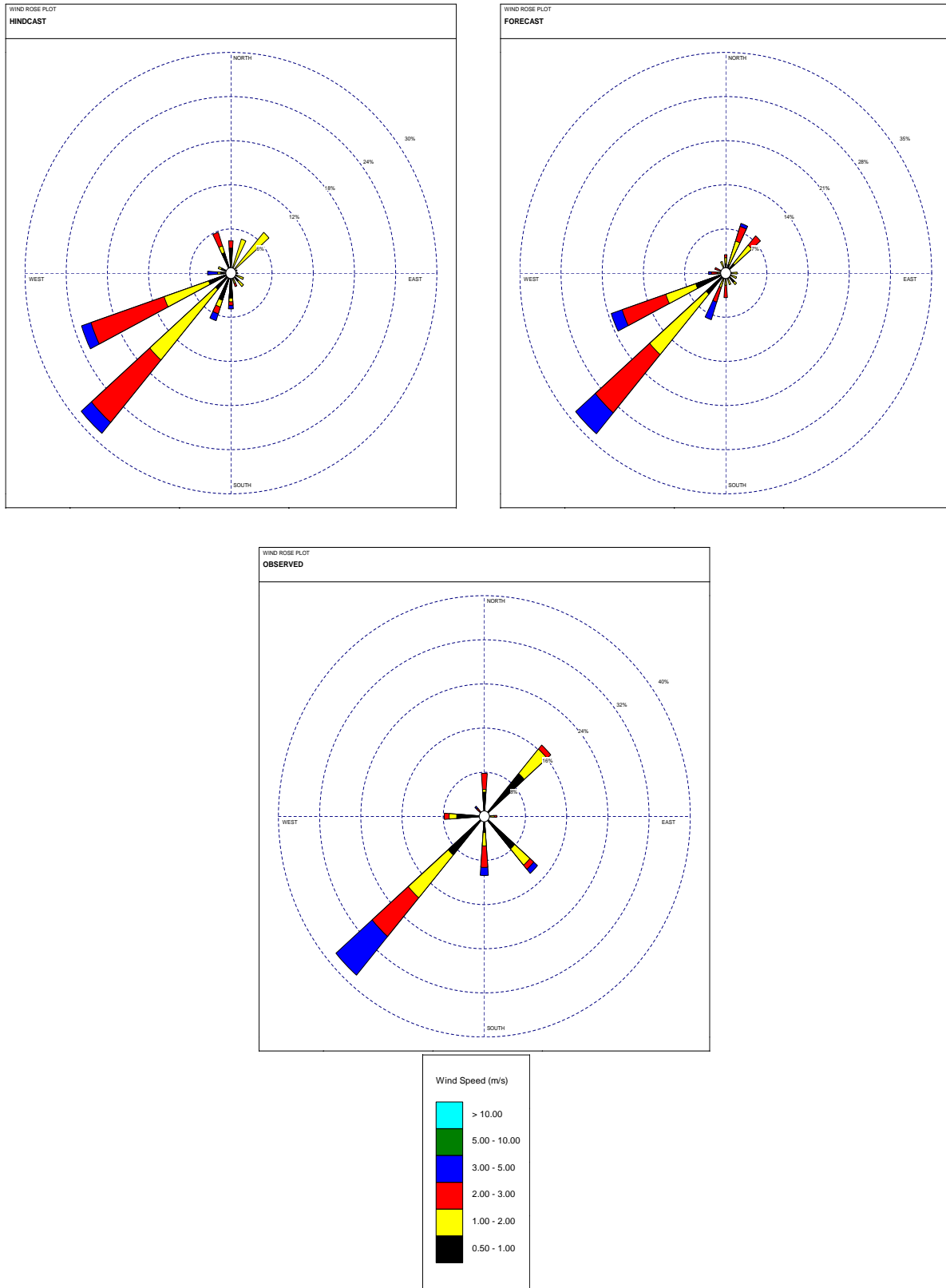


Figure 14: Windrose diagrams showing observed and modelled surface winds for the duration of the summer simulation at MoF-2056 station.

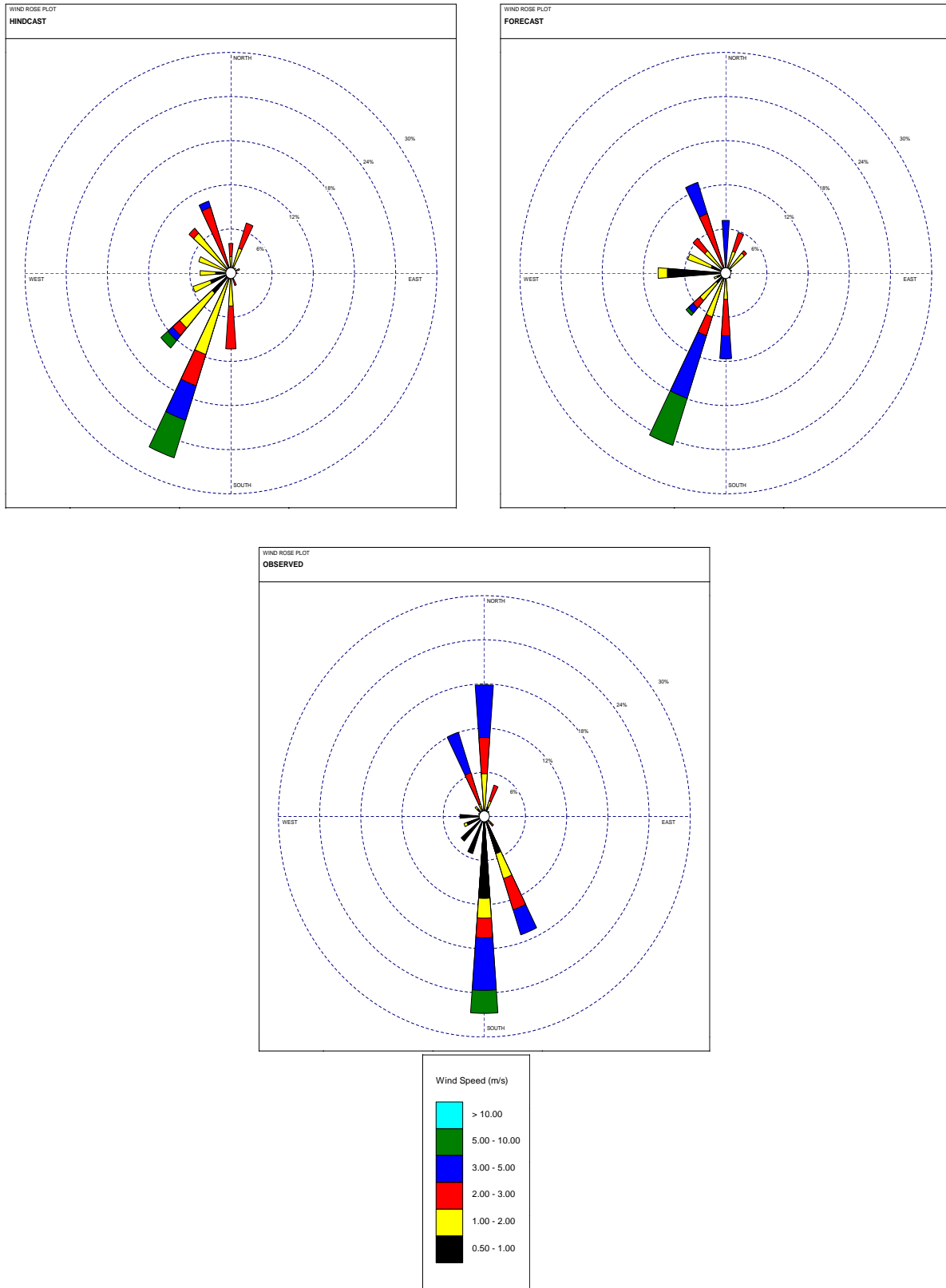


Figure 15: Windrose diagrams showing observed and modelled surface winds for the duration of the winter simulation at MoTH-21091 station.

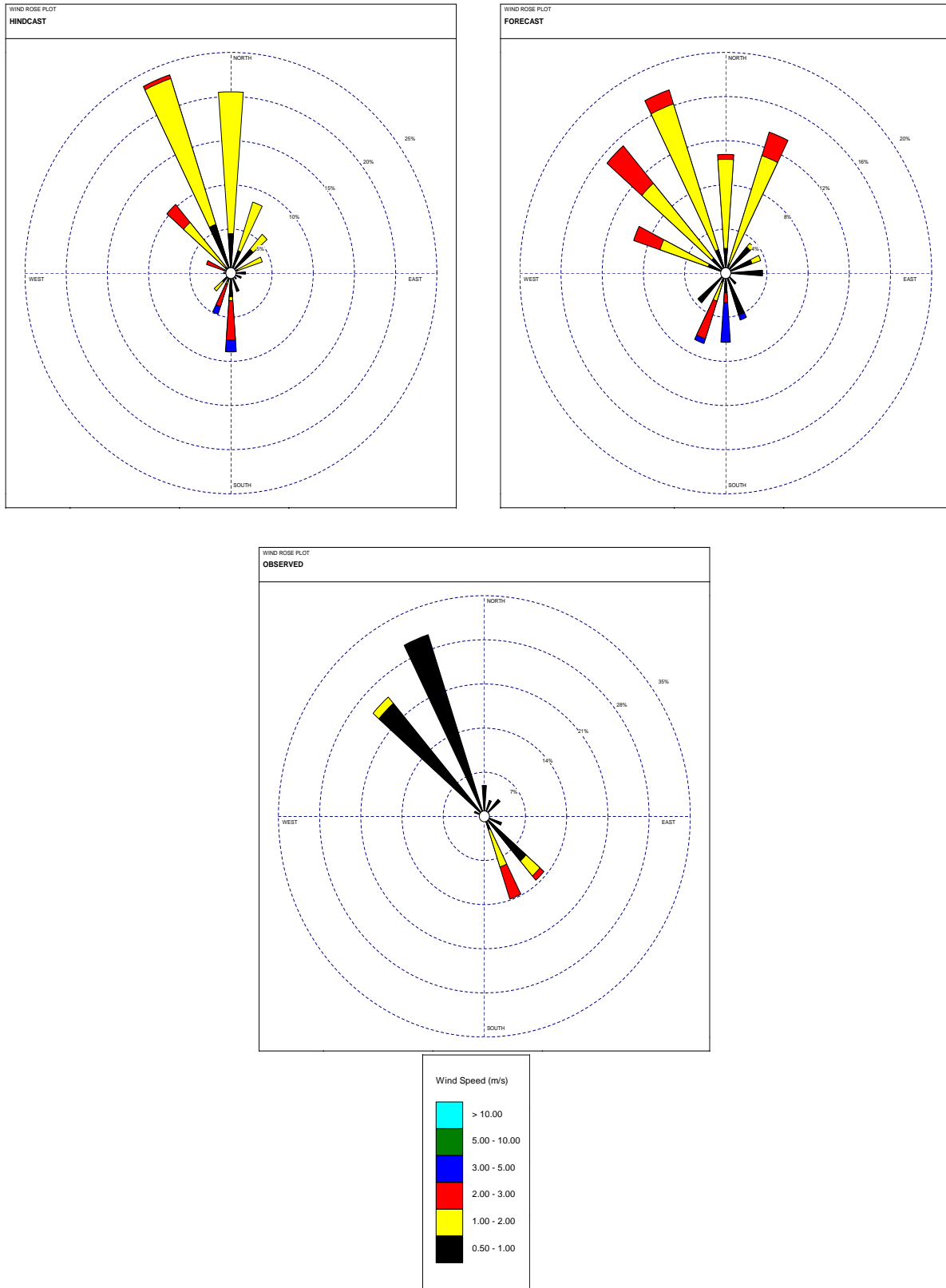


Figure 16: Windrose diagrams showing observed and modelled surface winds for the duration of the winter simulation at MoTH-33099 station.

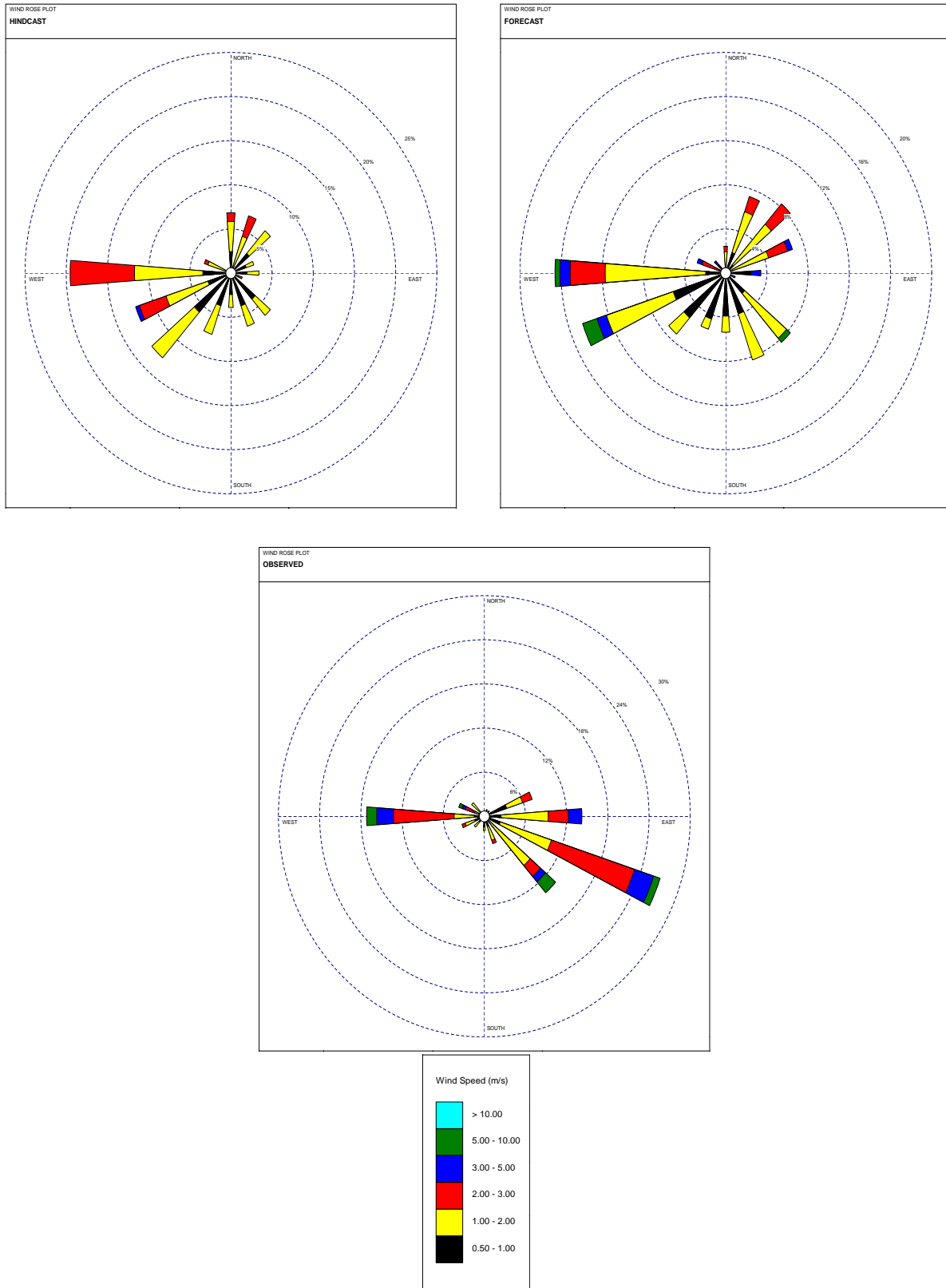


Figure 17: Windrose diagrams showing observed and modelled surface winds for the duration of the summer simulation at WLAP-M116003 station.

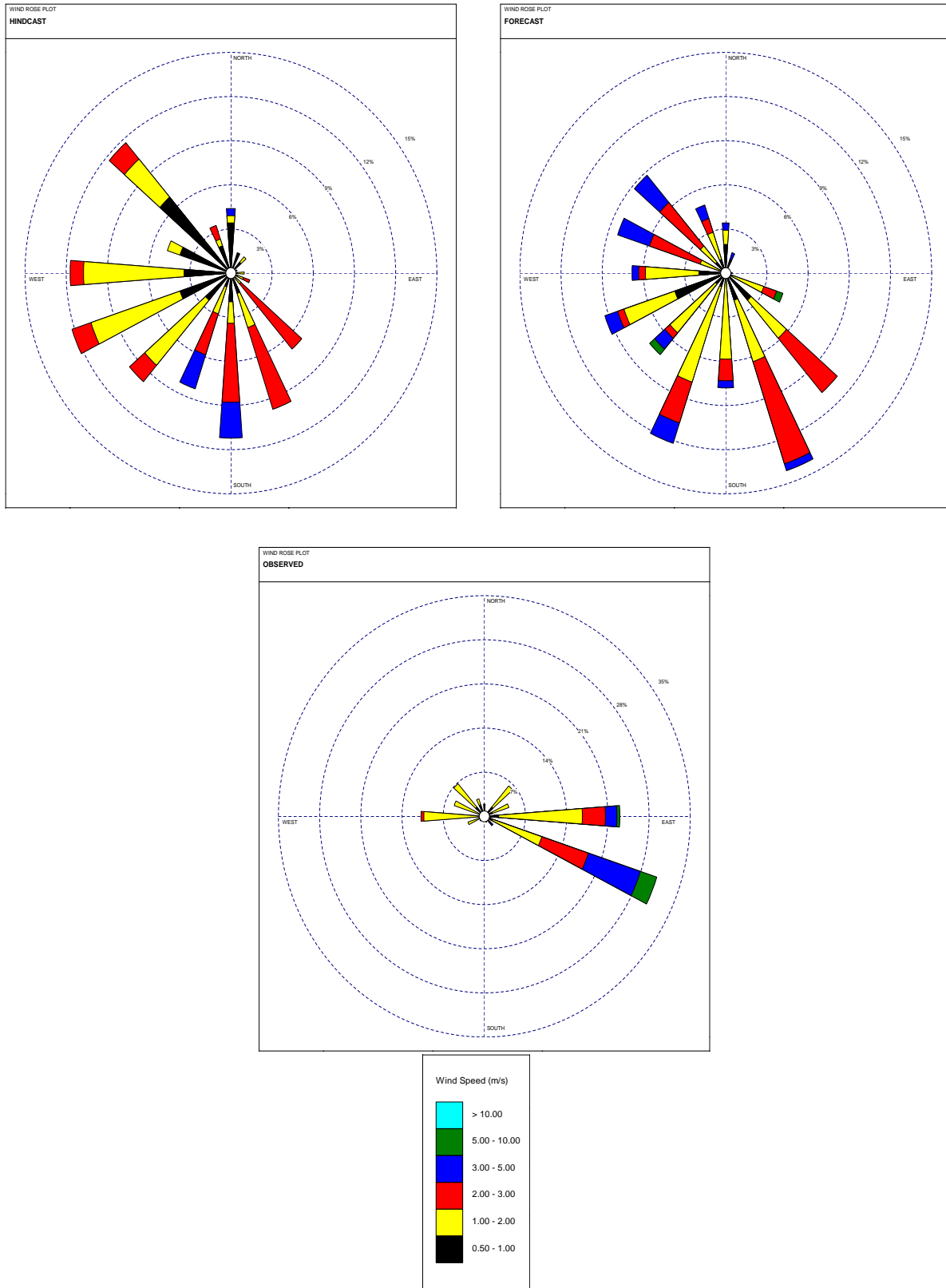


Figure 18: Windrose diagrams showing observed and modelled surface winds for the duration of the summer simulation at EC-WJV station.

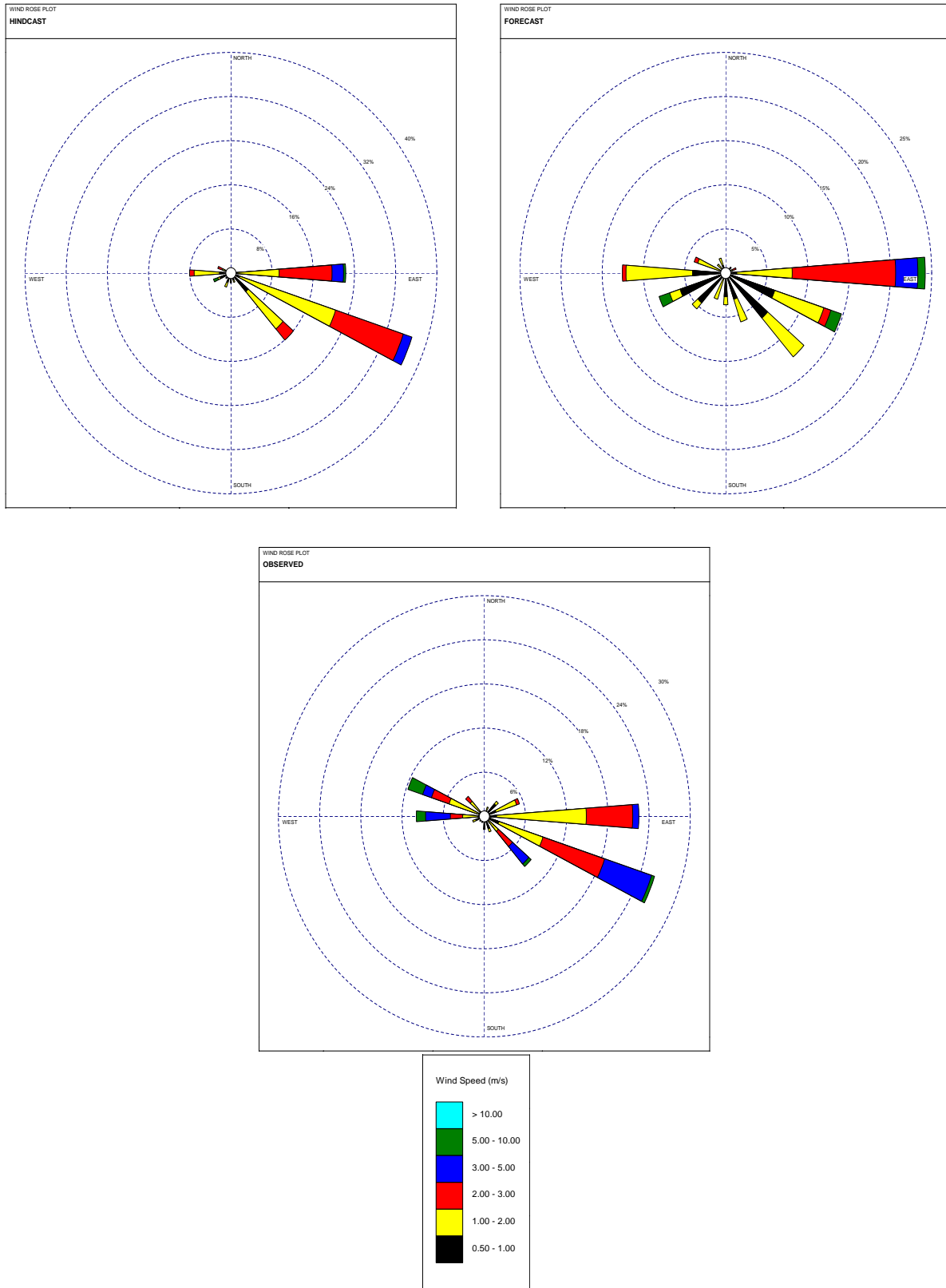


Figure 19: Windrose diagrams showing observed and modelled surface winds for the duration of the winter simulation at WLAP-M116003 station.

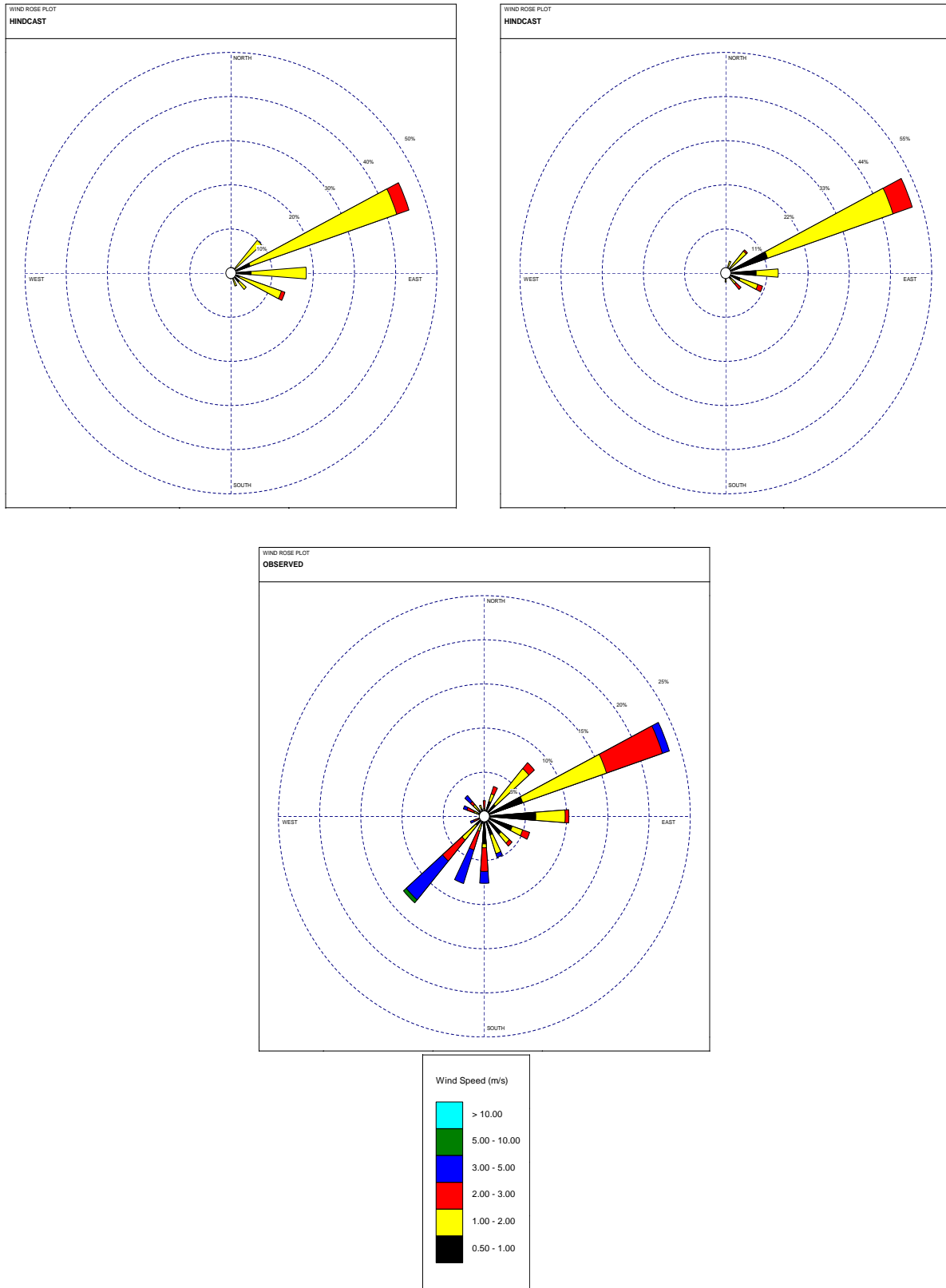


Figure 20: Windrose diagrams showing observed and modelled surface winds for the duration of the winter simulation at WLAP-M112070 station.

9 Appendix C: Significance Testing

WINTER MODELING PERIOD

Table 1: Correlation coefficients (r) measuring the degree of linear correlation between the observed and modeled values. Correlation coefficients that are not significantly different than 0 at the 95% confidence level are highlighted. Interpretation: a correlation coefficient (r) of 0.36 implies that only 13% (r^2) of the observed values can be explained by the model.

	Station	Sample n	U vector	V vector	Temp.	Speed
Winter Hindcast	WLAP1	222	0.36	-0.08	0.80	0.13
	EC-YKA	224	0.17	-0.05	0.76	0.10
	MoT-33099	223	0.31	0.84	0.78	0.64
	EC-WJV	222	0.24	0.06	0.74	0.12
	MoT-23097	223	0.31	0.20	0.77	0.17
	WLAP 2	224	0.23	0.24	0.66	0.05
	EC-YLW	224	-0.45	0.33	0.72	0.40
	EC-WUS	224	0.27	-0.16	0.72	0.19
	MoT-21091	223	-0.12	0.76	0.75	0.62
	Combined	2010	0.24	0.42	0.76	0.33
Winter Forecast	WLAP1	222	0.24	-0.05	0.76	0.26
	EC-YKA	224	0.07	-0.03	0.72	0.11
	MoT-33099	223	0.31	0.89	0.82	0.76
	EC-WJV	222	0.17	0.20	0.71	0.09
	MoT-23097	223	0.16	0.15	0.77	0.26
	WLAP 2	224	0.04	0.08	0.65	-0.09
	EC-YLW	224	-0.35	0.27	0.69	0.41
	EC-WUS	224	0.31	0.04	0.72	-0.06
	MoT-21091	223	-0.08	0.79	0.76	0.49
	Combined	2010	0.17	0.44	0.74	0.28

Table 2: Statistically significant differences between correlation coefficients are highlighted and labeled as to whether hindcast or forecast conditions exhibit larger correlations (stronger relationships). Blank cells represent conditions where there is no statistically significant difference between correlation coefficients for the winter season hindcasts and forecasts at the 95% confidence level.

	Station	Sample n	U vector	V vector	Temp.	Speed
Difference	WLAP1	222				
	EC-YKA	224				
	MoT-33099	223		Hindcast		Forecast
	EC-WJV	222				
	MoT-23097	223	Hindcast			
	WLAP 2	224	Hindcast			
	EC-YLW	224				
	EC-WUS	224				Hindcast
	MoT-21091	223				Hindcast
	Combined	2010	Hindcast			

SUMMER MODELING PERIOD

Table 3: Statistically significant differences between correlation coefficients are highlighted and labeled as to whether hindcast or forecast conditions exhibit larger correlations (stronger relationships). Blank cells represent conditions where there is no statistically significant difference between correlation coefficients for the summer season hindcasts and forecasts at the 95% confidence level.

	Station	Sample n	U vector	V vector	Temp.	Speed
Summer	MOF-2033	205	0.09	0.43	0.91	0.51
Hindcast	MoF-2051	205	0.54	0.66	0.92	0.24
	MoF-2035	205	0.20	0.54	0.92	0.61
	WLAP 1	203	-0.08	-0.11	0.89	0.28
	EC YKA	204	0.16	0.02	0.85	0.05
	MoF 2056	205	0.62	0.57	0.94	0.62
	EC-WJV	204	0.28	-0.05	0.90	-0.06
	MoF-2026	205	0.50	0.44	0.90	0.21
	WLAP 2	204	0.42	0.39	0.89	0.11
	EC YLW	205	0.19	0.14	0.86	0.05
	EC WUS	205	0.35	-0.04	0.86	-0.22
		Combined	2251	0.216	0.357	0.89
Summer	MOF-2033	205	-0.03	0.29	0.88	0.53
Forecast	MoF-2051	205	0.43	0.64	0.94	0.17
	MoF-2035	205	0.29	0.49	0.91	0.62
	WLAP 1	203	0.05	-0.02	0.90	0.31
	EC YKA	204	0.03	0.07	0.87	0.13
	MoF 2056	205	0.51	0.56	0.94	0.60
	EC-WJV	204	0.50	0.15	0.92	-0.13
	MoF-2026	205	0.38	0.04	0.89	0.19
	WLAP 2	204	0.32	0.31	0.92	0.14
	EC YLW	205	0.15	-0.10	0.87	0.12
	EC WUS	205	0.21	0.14	0.89	-0.24
		Combined	2251	0.21	0.32	0.90

Table 4: Statistically significant differences between correlation coefficients are highlighted and labeled as to whether hindcast or forecast conditions exhibit larger correlations (stronger relationships). Blank cells represent conditions where there is no statistically significant difference between correlation coefficients for the summer season hindcasts and forecasts at the 95% confidence level.

	Station	Sample n	U vector	V vector	Temp.	Speed
Summer Hindcast	MOF-2033	205				
	MoF-2051	205				
	MoF-2035	205				
	WLAP 1	203				
	EC YKA	204				
	MoF 2056	205				
	EC-WJV	204		Forecast		
	MoF-2026	205			Hindcast	
	WLAP 2	204				
	EC YLW	205				
	EC WUS	205				
	Combined	2251				

Table 5: Statistically significant differences between correlation coefficients for the hindcasts in the winter and summer seasons are highlighted and labeled as to whether hindcast or forecast conditions exhibit larger correlations (stronger relationships). Blank cells represent conditions where there is no statistically significant difference between correlation coefficients at the 95% confidence level.

	Station	Sample n	U vector	V vector	Temp.	Speed
Winter vs Summer	WLAP 1	205	Winter	Summer	Summer	Summer
	EC YKA	205		Summer	Summer	
Hindcast	WLAP 2	205	Winter	Summer	Summer	
	EC YLW	203	Summer	Winter	Summer	Winter
	EC WUS	204			Summer	Winter

Table 6: Statistically significant differences between correlation coefficients for the forecasts in the winter and summer seasons are highlighted and labeled as to whether hindcast or forecast conditions exhibit larger correlations (stronger relationships). Blank cells represent conditions where there is no statistically significant difference between correlation coefficients at the 95% confidence level.

	Station	Sample n	U vector	V vector	Temp.	Speed
Winter vs Summer	WLAP 1	205	Winter		Summer	
	EC YKA	205			Summer	
Forecast	WLAP 2	205	Summer	Summer	Summer	
	EC YLW	203	Summer	Winter	Summer	Winter
	EC WUS	204			Summer	

Table 7: Error band for 95% confidence level for summer forecast data. Interpretation: Model results from WLAP-1 would be recorded as $x_m \pm 1.85 \text{ m s}^{-1}$ for wind speed and $x_m \pm 166.6^\circ$ for wind direction.

	U vector	V vector	Temp.	Speed	Direction
WLAP-1	1.85	2.00	5.71	1.51	166.56
EC-YKA	3.28	1.40	9.98	1.55	121.97
EC-WJV	2.73	3.00	9.26	1.96	149.67
WLAP-2	2.31	2.13	9.83	1.66	163.87
MoF-2053	3.08	2.24	8.94	1.89	155.11
MoF-2051	3.23	4.16	10.04	2.39	161.24
MoF-2035	1.60	2.48	10.62	1.98	100.94
MoF-2056	2.54	2.45	9.52	1.85	166.51
MoF-2026	3.21	2.34	10.01	2.43	127.41
EC-YLW	2.64	2.37	9.85	2.13	142.18
EC-WUS	3.50	3.02	8.61	2.77	180.00

Table 8: Error band for 95% confidence level for summer hindcast data. Interpretation: Model results from WLAP-1 would be recorded as $x_m \pm 2.19 \text{ m s}^{-1}$ for wind speed and $x_m \pm 184.2^\circ$ for wind direction.

	U vector	V vector	Temp.	Speed	Direction
WLAP-1	2.19	1.66	9.99	1.25	180.00
EC-YKA	2.66	1.19	10.32	1.16	107.79
EC-WJV	1.79	2.69	10.21	1.87	155.01
WLAP-2	1.82	1.67	10.33	1.14	149.56
MoF-2053	2.16	2.25	9.79	1.37	143.29
MoF-2051	2.36	4.36	10.51	2.34	181.31
MoF-2035	1.47	2.14	11.01	1.69	123.37
MoF-2056	2.41	2.20	9.92	1.74	172.85
MoF-2026	2.62	2.55	9.98	2.43	114.21
EC-YLW	2.03	2.00	10.42	1.63	115.48
EC-WUS	3.19	1.93	8.84	2.00	180.00

Table 9: Error band for 95% confidence level for winter forecast data. Interpretation: Model results from WLAP-1 would be recorded as $x_m \pm 3.39 \text{ m s}^{-1}$ for wind speed and $x_m \pm 148.1^\circ$ for wind direction.

	U vector	V vector	Temp.	Speed	Direction
WLAP-1	3.39	1.06	5.92	2.29	148.14
EC-WJV	1.58	2.53	5.23	1.64	158.22
MoTH-33094	2.01	5.07	5.47	2.99	180.00
MoTH-23097	1.93	2.27	5.37	1.95	165.40
MoTH-21091	1.51	2.82	5.89	1.67	251.45
EC-YKA	2.94	1.75	6.21	1.74	136.45
WLAP-2	1.19	1.27	6.72	1.03	83.89
EC-YLW	1.74	1.71	6.79	1.43	180.00
EC-WUS	6.56	2.08	5.55	4.71	180.00

Table 10: Error band for 95% confidence level for winter hindcast data. Interpretation: Model results from MoTH-23097 would be recorded as $x_m \pm 1.85 \text{ m s}^{-1}$ for wind speed and $x_m \pm 166.6^\circ$ for wind direction.

	U vector	V vector	Temp.	Speed	Direction
MoTH-23097	1.85	2.00	5.71	1.51	166.56
WLAP-2	0.97	1.28	6.65	0.80	78.13
WLAP-1	2.88	1.10	5.94	1.79	122.96
EC-WJV	1.74	2.22	5.63	1.37	135.96
EC-YKA	1.86	2.00	5.72	1.51	164.77
MoTH-33094	1.84	4.18	6.11	2.68	172.10
MoTH-21091	1.30	2.52	6.33	1.40	180.00
EC-YLW	1.83	1.77	6.5	1.45	163.71
EC-WUS	2.63	1.51	5.33	1.35	180.00

Table 11: Percentage (%) of modeled wind direction values that are within a given error band measured in degrees for summer forecast and hindcast results. Interpretation: 7.88% of modeled values for WLAP-1 are within $\pm 22.5^\circ$ of the observed.

	Forecast				Hindcast			
	$\pm 22.5^\circ$	$\pm 45^\circ$	$\pm 90^\circ$	$\pm 180^\circ$	$\pm 22.5^\circ$	$\pm 45^\circ$	$\pm 90^\circ$	$\pm 180^\circ$
WLAP-1	7.88	16.26	42.86	99.51	5.42	19.21	36.95	99.51
EC-YKA	3.43	12.25	22.06	99.51	5.39	12.25	22.06	99.51
EC-WJV	8.33	30.39	54.41	99.51	8.33	21.57	41.67	99.51
WLAP-2	28.43	39.71	71.57	99.51	25.98	50.49	77.94	99.51
MoF-2053	22.93	39.51	69.27	99.51	32.20	48.29	75.12	99.51
MoF-2051	36.59	54.63	81.95	99.51	34.63	53.17	80.49	99.51
MoF-2035	31.71	54.15	76.10	99.51	31.71	50.24	77.07	99.51
MoF-2056	42.44	64.88	80.98	99.51	41.46	63.41	80.98	99.51
MoF-2026	13.66	33.17	58.05	99.51	18.05	39.51	67.32	99.51
EC-YLW	4.88	15.61	34.15	99.51	13.17	21.46	37.07	99.51
EC-WUS	26.34	50.73	70.73	99.51	24.39	46.83	65.85	99.51

Table 12. Percentage (%) of modeled wind direction values that are within a given error band measured in degrees for winter forecast and hindcast results. Interpretation: 9.87% of modeled values for MoTH-23097 are within $\pm 22.5^\circ$ of the observed.

	Forecast				Hindcast			
	$\pm 22.5^\circ$	$\pm 45^\circ$	$\pm 90^\circ$	$\pm 180^\circ$	$\pm 22.5^\circ$	$\pm 45^\circ$	$\pm 90^\circ$	$\pm 180^\circ$
MoTH-23097	9.87	20.18	40.81	99.51	12.50	28.13	51.79	99.51
WLAP-2	28.57	45.09	61.61	99.51	31.56	50.67	64.89	99.51
WLAP-1	24.77	42.79	56.31	99.51	39.64	63.06	76.58	99.51
EC-WJV	11.71	18.02	51.80	99.51	2.70	18.47	45.05	99.51
EC-YKA	11.16	18.75	41.07	99.51	12.11	27.8	51.57	99.51
MoTH-33094	39.46	68.61	82.96	99.51	33.18	65.92	87.44	99.51
MoTH-21091	31.39	53.81	82.51	99.51	30.49	60.99	86.55	99.51
EC-YLW	14.73	27.68	41.07	99.51	16.52	29.02	45.54	99.51
EC-WUS	29.02	46.43	69.20	99.51	23.21	43.30	56.70	99.51

Table 13. Percentage of modeled temperature values that are within a given error band measured in degrees for summer forecast and hindcast results. Interpretation: 30.5% of modeled temperature values for WLAP-1 are within 1° of the observed.

	Forecast				Hindcast			
	1°	2°	3°	5°	1°	2°	3°	5°
WLAP-1	30.54	52.71	72.91	92.12	34.98	63.55	79.31	92.12
EC-YKA	30.88	49.02	68.63	89.71	25.00	49.51	67.65	92.16
EC-WJV	21.57	36.27	58.33	94.61	32.35	52.45	71.57	93.63
WLAP-2	36.76	66.67	87.25	99.02	19.61	43.14	65.20	89.22
MoF-2053	22.44	44.39	66.83	93.66	29.27	54.15	77.07	92.68
MoF-2051	35.61	66.83	91.71	100	33.66	64.39	82.93	98.54
MoF-2035	36.59	59.02	68.78	85.37	30.73	60.49	79.02	91.71
MoF-2056	45.37	75.61	91.22	99.02	43.90	70.73	90.24	99.51
MoF-2026	22.44	43.41	69.76	96.59	39.51	64.39	77.56	98.54
EC-YLW	21.46	35.12	52.68	84.39	25.37	47.80	64.88	82.93
EC-WUS	31.71	57.56	79.02	98.05	33.17	58.54	78.54	94.63

Table 14. Percentage of modeled temperature values that are within a given error band measured in degrees for winter forecast and hindcast results. Interpretation: 24.66% of modeled temperature values are within 1° of the observed.

	Forecast				Hindcast			
	1°	2°	3°	5°	1°	2°	3°	5°
MoTH-23097	24.66	35.87	46.19	56.95	18.30	35.71	47.32	56.70
WLAP-2	15.63	31.25	45.09	67.41	16.44	34.67	49.33	67.11
WLAP-1	11.71	22.07	35.59	46.40	12.61	23.87	37.84	45.95
EC-WJV	9.46	18.02	27.03	38.74	7.21	17.57	27.48	39.64
EC-YKA	14.73	22.77	36.61	54.46	18.39	35.87	47.53	56.95
MoTH-33094	9.42	13.00	13.45	19.28	7.17	13.00	16.14	18.39
MoTH-21091	6.73	9.42	11.66	19.28	5.38	9.87	13.00	21.08
EC-YLW	12.95	28.57	44.64	58.93	15.63	33.93	48.21	57.59
EC-WUS	21.43	34.82	43.30	58.48	20.54	33.48	42.41	59.38

Table 15. Percentage of modeled wind speed values that are within a given error band measured in degrees for summer forecast and hindcast results. Interpretation: 56.16% of modeled values for WLAP-1 are within 1 m s^{-1} of the observed values.

	Forecast				Hindcast			
	1 m s^{-1}	2 m s^{-1}	3 m s^{-1}	5 m s^{-1}	1 m s^{-1}	2 m s^{-1}	3 m s^{-1}	5 m s^{-1}
WLAP-1	56.16	85.22	94.09	99.51	57.14	88.18	95.07	99.01
EC-YKA	31.86	40.69	45.59	49.02	31.86	42.65	44.61	49.02
EC-WJV	39.71	75.49	88.73	97.55	50.98	75.98	86.76	98.04
WLAP-2	53.92	86.27	92.16	99.02	56.37	83.33	94.61	99.02
MoF-2053	18.05	39.02	48.78	51.71	17.56	44.39	51.71	52.20
MoF-2051	42.44	79.02	93.17	98.05	47.80	79.02	93.66	99.02
MoF-2035	50.24	71.22	77.56	78.54	53.17	71.71	78.05	78.54
MoF-2056	54.63	74.63	81.95	81.95	41.46	63.41	80.98	99.51
MoF-2026	29.27	57.07	73.17	79.51	25.37	59.02	71.71	80.49
EC-YLW	32.20	48.29	55.59	58.54	35.61	50.73	55.61	58.54
EC-WUS	44.88	76.10	93.66	98.05	46.83	77.56	96.59	99.51

Table 16. Percentage of modeled wind speed values that are within a given error band measured in degrees for winter forecast and hindcast results. Interpretation: 63.68% of modeled values for MoTH-23097 are within 1 m s^{-1} of the observed values.

	Forecast				Hindcast			
	1 m s^{-1}	2 m s^{-1}	3 m s^{-1}	5 m s^{-1}	1 m s^{-1}	2 m s^{-1}	3 m s^{-1}	5 m s^{-1}
MoTH-23097	63.68	88.34	95.96	96.86	62.50	89.73	95.54	96.88
WLAP-2	56.70	87.50	95.68	99.11	63.56	89.78	95.56	99.11
WLAP-1	52.70	79.28	92.34	98.65	56.76	79.73	90.99	98.65
EC-WJV	57.66	78.83	82.43	83.78	57.66	77.93	81.98	83.78
EC-YKA	25.45	40.18	44.64	46.43	62.78	90.13	95.96	97.31
MoTH-33094	64.57	88.34	96.41	97.76	50.22	86.10	95.96	97.76
MoTH-21091	39.01	72.20	75.78	75.78	52.02	73.54	75.78	75.78
EC-YLW	41.52	51.34	53.13	55.80	39.73	51.34	54.46	55.80
EC-WUS	53.57	78.57	85.27	89.73	66.52	91.07	96.88	98.21

Table 17. Percentage of modeled values that are within the correct sector for the winter season.

	Forecast		Hindcast	
	East West Sector	North South Sector	East West Sector	North South Sector
WLAP-1	58.62	56.16	52.22	59.61
EC-YKA	46.08	33.33	42.65	32.35
EC-WJV	64.71	65.69	57.35	67.16
WLAP-2	70.59	73.04	75.00	79.41
MoF-2053	62.93	71.71	67.80	71.22
MoF-2051	80.98	75.61	78.54	77.07
MoF-2035	84.88	75.61	88.29	79.51
MoF-2056	89.27	80.00	88.29	81.95
MoF-2026	66.34	64.88	75.12	66.34
EC-YLW	55.61	41.95	55.12	44.39
EC-WUS	71.71	79.02	68.78	75.61

Table 18. Percentage of modeled values that are within the correct sector for the summer season.

	Forecast		Hindcast	
	East West Sector	North South Sector	East West Sector	North South Sector
MoTH-23097	58.74	36.32	62.05	41.96
WLAP-2	58.04	49.55	62.22	58.67
WLAP-1	53.15	63.06	75.68	64.41
EC-WJV	40.54	56.76	43.69	53.60
EC-YKA	59.82	29.02	62.33	42.15
MoTH-33094	70.40	78.92	66.37	82.41
MoTH-21091	52.02	84.75	54.26	83.41
EC-YLW	31.70	44.20	49.11	50.00
EC-WUS	66.96	52.68	58.04	47.32

Table 19. Correlation coefficients (r) for the summer hindcast using data for winds greater than the threshold wind speeds of 1, 2 and 3 m s^{-1} . Interpretation: the correlation coefficient between WLAP-1 modeled and observed values of Uvector is -0.07 for winds greater than 1 m s^{-1} .

	Threshold	WLAP-1	EC-YKA	EC-WJV	WLAP-2	MoF-2033	MoF-2051	MoF-2035	MoF-2056	MoF-2026	EC-YLW	EC-WUS
U vector	1	-0.07	0.19	0.29	0.42	-0.24	0.54	0.14	0.63	0.65	0.21	0.35
	2	-0.05	0.42	-0.06	0.42	--	0.55	-0.06	0.45	0.68	0.27	0.45
	3	0.11	-0.04	0.04	-0.04	--	0.11	-0.18	-0.16	-0.40	-0.06	0.26
V vector	1	-0.10	0.03	-0.08	0.38	0.20	0.69	0.48	0.61	0.64	0.18	-0.04
	2	0	-0.04	-0.12	0.43	--	0.73	0.40	0.57	0.77	0.13	-0.17
	3	0.02	0.05	-0.0	0.60	--	0.77	0.24	0.45	0.76	0.27	-0.28
Temp	1	0.87	0.84	0.90	0.88	0.83	0.92	0.96	0.95	0.92	0.86	0.85
	2	0.88	0.85	0.82	0.87	--	0.92	0.96	0.96	0.88	0.93	0.78
	3	0.82	0.85	0.85	0.81	--	0.94	0.98	0.97	0.84	0.95	0.84
Speed	1	0.25	0.13	-0.15	0.08	-0.11	0.23	0.36	0.43	-0.14	-0.08	-0.25
	2	0.24	0.01	0.02	-0.07	--	0.13	0.17	0.18	-0.07	0.45	-0.26
	3	0.18	0.03	0.05	0.04	--	-0.02	-0.06	0.03	-0.03	0.45	-0.13
East West	1	0.38	0.21	0.44	0.61	0.08	0.60	0.29	0.54	0.28	0.34	0.6
	2	0.20	0.12	0.11	0.34	--	0.35	0.21	0.30	0.10	0.10	0.29
	3	0.08	0.07	0.08	0.06	--	0.20	0.11	0.13	0.05	0.08	0.16
North South	1	0.44	0.22	0.48	0.68	0.13	0.60	0.31	0.50	0.23	0.29	0.67
	2	0.28	0.10	0.22	0.44	--	0.38	0.25	0.29	0.07	0.11	0.31
	3	0.09	0.5	0.16	0.16	--	0.19	0.11	0.13	0.01	0.07	0.21
Count	1	175	100	172	191	29	169	90	126	90	118	205
	2	96	43	59	115	1	98	63	71	39	28	96
	3	33	20	44	35	0	49	30	30	14	20	60

Table 20. Correlation coefficients (r) for the summer forecast using data for winds greater than the threshold wind speeds of 1, 2 and 3 m s^{-1} . Interpretation: the correlation coefficient between WLAP-1 modeled and observed values of Uvector is 0.06 for winds greater than 1 m s^{-1} .

	Threshold	WLAP-1	EC-YKA	EC-WJV	WLAP-2	MoF-2033	MoF-2051	MoF-2035	MoF-2056	MoF-2026	EC-YLW	EC-WUS
Uve ctor	1	0.06	0.02	0.50	0.32	-0.17	0.43	0.35	0.49	0.43	0.21	0.21
	2	0.11	0.14	0.29	0.29	--	0.42	0.40	0.31	0.34	0.46	0.14
	3	0.34	0.33	0.30	-0.04	--	0.02	0.13	0.07	-0.27	0.36	0.04
Vve ctor	1	0	0.10	0.14	0.30	0.11	0.66	0.33	0.59	0.03	-0.11	0.13
	2	0.13	0.12	0.13	0.64	--	0.74	0.34	0.54	0.09	-0.37	0.23
	3	0.32	0.21	0.15	0.42	--	0.78	0.31	0.47	0.59	0.45	-0.06
Tem p	1	0.88	0.87	0.90	0.92	0.78	0.93	0.96	0.96	0.91	0.88	0.88
	2	0.90	0.87	0.89	0.91	--	0.94	0.96	0.97	0.86	0.95	0.58
	3	0.86	0.87	0.92	0.92	--	0.93	0.98	0.97	0.88	0.96	0.87
Spee d	1	0.31	0.12	-0.26	0.11	-0.10	0.12	0.17	0.38	-0.12	0.05	-0.26
	2	0.32	0.04	0.07	-0.05	--	0	0.01	0.15	0.02	-0.04	0.12
	3	0.50	-0.09	0.09	0.09	--	0	0.11	0.04	-0.02	-0.05	0.15
East West	1	0.43	0.21	0.49	0.58	0.08	0.63	0.29	0.52	0.26	0.30	0.63
	2	0.23	0.11	0.15	0.33	0.01	0.38	0.22	0.29	0.11	0.08	0.31
	3	0.09	0.06	0.14	0.09	0	0.2	0.10	0.13	0.06	0.06	0.2
Nort h	1	0.39	0.22	0.49	0.59	0.11	0.59	0.30	0.48	0.2	0.25	0.70
	2	0.25	0.11	0.25	0.40	0.005	0.39	0.25	0.29	0.05	0.06	0.33
	3	0.07	0.06	0.19	0.16	0	0.2	0.14	0.13	0.01	0.04	0.21
Cou nt	1	175	100	172	191	29	169	90	126	90	118	205
	2	96	43	59	115	1	98	63	71	39	28	96
	3	33	20	44	35	0	49	30	30	14	20	60

Table 21. Correlation coefficients (r) for the winter forecast using data for winds greater than the threshold wind speeds of 1, 2 and 3 m s⁻¹. Interpretation: the correlation coefficient between MoTH-23097 modeled and observed values of Uvector is 0.16 for winds greater than 1 m s⁻¹.

	Threshold	MoTH-23097	WLAP-2	WLAP-1	EC-WJV	EC-YKA	MoTH-33094	MoTH-21091	EC-YLW	EC-WUS
Uve ctor	1	0.16	0.05	0.25	0.22	-0.0	0.30	-0.44	-0.39	0.34
	2	0.08	0.04	0.29	0.19	0.22	0.33	-0.02	-0.38	0.43
	3	0.06	-0.20	-0.51	-0.24	-	-0.49	--	0.04	0.04
Vve ctor	1	0.21	0.07	-0.07	0.24	0.03	0.92	0.68	0.35	0.06
	2	0.51	0.06	-0.12	0.05	-0.17	0.95	0.34	0.46	0.07
	3	0.78	-0.02	-0.36	0.8	-	0.97	-0.78	0.48	0.03
Tem p	1	0.82	0.68	0.76	0.75	0.86	0.78	0.87	0.66	0.74
	2	0.85	0.71	0.83	0.82	0.91	0.76	0.90	0.80	0.77
	3	0.95	0.54	0.89	0.80	-	0.79	0.99	0.80	0.80
Spee d	1	0.45	-0.15	0.24	0.19	0.18	0.65	0.72	0.28	-0.01
	2	0.64	-0.26	0.20	0.15	-	0.71	0.39	-0.25	0.13
	3	0.64	-0.37	0.42	-0.09	-	0.74	--	-0.39	-0.03
East Wes	1	0.30	0.37	0.49	0.28	0.17	0.72	0.08	0.17	0.61
	2	0.09	0.13	0.28	0.07	0.04	0.32	0.02	0.04	0.29
	3	0.02	0.01	0.09	0.05	0	0.23	00	0.02	0.18
Nort h	1	0.17	0.347	0.55	0.36	0.11	0.57	0.14	0.28	0.46
	2	0.04	0.18	0.32	0.09	0.04	0.45	0.06	0.10	0.16
	3	0.02	0.06	0.12	0.07	0	0.32	0.01	0.07	0.10
Cou nt	1	129	184	195	134	62	138	38	120	200
	2	40	85	111	26	21	104	14	36	81
	3	7	35	49	18	0	72	3	25	52

Table 22. Correlation coefficients (r) for the winter hindcast using data for winds greater than the threshold wind speeds of 1, 2 and 3 m s⁻¹. Interpretation: the correlation coefficient between MoTH-23097 modeled and observed values of Uvector is 0.35 for winds greater than 1 m s⁻¹.

	Threshold	MoTH-23097	WLAP-2	WLAP-1	EC-WJV	EC-YKA	MoTH-33094	MoTH-21091	EC-YLW	EC-WUS
Uve ctor	1	0.35	0.30	0.38	0.25	0.35	0.32	-0.29	-0.48	0.27
	2	0.36	0.27	0.44	0.44	0.36	0.33	-0.03	-0.43	0.23
	3	-0.47	0.26	-0.52	-0.06	-0.47	-0.47	--	0.13	0.07
Vve ctor	1	0.28	0.27	-0.11	0.03	0.28	0.88	0.67	0.45	-0.16
	2	0.49	0.35	-0.19	-0.08	0.49	0.91	0.46	0.65	-0.30
	3	0.66	0.01	-0.42	0.01	0.66	0.91	0.30	0.66	-0.32
Tem p	1	0.85	0.72	0.81	0.8	0.85	0.72	0.91	0.70	0.75
	2	0.90	0.76	0.85	0.9	0.90	0.72	0.78	0.78	0.79
	3	0.98	0.56	0.89	0.87	0.98	0.75	0.96	0.78	0.79
Spee d	1	0.31	-0.14	0.14	0.06	0.31	0.55	0.72	0.34	0.23
	2	0.60	0.15	0.19	-0.01	0.60	0.62	0.48	-0.19	0.04
	3	0.82	0.08	0.54	-0.33	0.82	0.66	--	-0.25	-0.17
East Wes	1	0.35	0.40	0.67	0.30	0.35	0.38	0.02	0.24	0.54
	2	0.10	0.14	0.37	0.07	0.10	0.29	0.00	0.05	0.24
	3	0.01	0.02	0.17	0.06	0.01	0.19	0.00	0.03	0.17
Nort h	1	0.22	0.42	0.56	0.35	0.22	0.56	0.14	0.31	0.42
	2	0.07	0.24	0.32	0.07	0.07	0.43	0.06	0.12	0.09
	3	0.02	0.08	0.11	0.07	0.02	0.30	0.01	0.09	0.05
Cou nt	1	129	154	195	134	129	138	38	120	200
	2	40	85	111	26	40	104	14	36	81
	3	7	35	49	18	7	72	3	25	52